KAMAN NUCLEAR DIVISION OF KAMAN CORPORATION
1700 GARDEN OF THE GODS ROAD, COLORADO SPRINGS, COLORADO 80907

THE EFFECTS OF THE AIR-EARTH INTERFACE ON THE PROPAGATION CONSTANTS OF A BURIED INSULATED CONDUCTOR

James H. Head

KN-785-70-6(R) 19 February 1970

This research supported by the Naval Electronic Systems Command through Office of Naval Research Contract No. N00014-66-C-0357, Task No. 321-013.

TABLE OF CONTENTS

ABSTRACT

In computing the response of a buried insulated conductor to an incident broad-band electromagnetic pulse, knowledge of the propagation constants for the buried conductor is required over the frequency range 10^{-2} Hz $\lesssim f \lesssim 10^{8}$ Hz. If the buried conductor is near the earth's surface, then the asymmetry introduced by the air-earth interface may be important in determining these propagation constants. The propagation constants in the absence of this interface can be found by straightforward methods. The present study presents a method for computing the propagation constants in the presence of this interface. Because of the frequency range of interest, the theory is developed without any approximations concerning the values of the electrical parameters of the media. The electric and magnetic fields in the neighborhood of the conductor are represented by two components: the primary (fundamental Transverse Magnetic mode) fields generated by the driving current and the secondary fields which arise from reflections of the primary fields from the air-earth interface. The reflected azimuthal magnetic field is found to be very small while the reflected longitudinal electric field is shown to be a significant part of the total field at the conductor surface. For two sets of soil parameters, the propagation constant is determined as a function of frequency for burial depths of 1m, 10m, 100m, and 1000m. Compared to the results for an insulated conductor buried in an infinite medium, the imaginary part of the propagation constant is shown to increase near some characteristic frequency by as much as 35%, and the real part to decrease by as much as 10%. Both the size of the change in the real and imaginary parts of the propagation constant and the frequency at which these changes take place are reduced with increased burial depth.

CHAPTER 1

INTRODUCTION

The analysis of buried conductors has most often been performed by neglecting the presence of the air-earth interface and treating a line source immersed in an infinite homogeneous environment[1]. While a complete solution to the actual problem is impossible (due to irregularities in the earth's surface and its lack of electrical homogeneity) the solution to the problem where the actual earth is replaced by a plane homogeneous semi-infinite solid is of considerable practical and theoretical interest. It is this problem that is considered here in detail.

The problem of a line source of alternating current situated near the interface separating homogeneous air from homogeneous earth has been studied by several authors[2-4]. These investigators derived expressions for the fields and propagation constants that were valid only at low frequencies since displacement currents were neglected. There are however cases of great importance where the frequency range is high enough that displacement currents are dominant and cannot be neglected. Perhaps the most thorough analysis has been performed by Wait[5], who treated a very simple driving field in detail.

In this paper a detailed study of the buried insulated conductor is presented. No specific reference is made to the actual characteristics of any medium, and the electrical properties of no medium are restricted in any sense. Specific attention is given to the determination of the axial propagation

constant over a wide frequency range (10^{-2} Hz $\leq f \lesssim 10^{8}$ Hz) as a function of the proximity of the interface.

In Chapter 2 the solution to the buried insulated conductor (neglecting the air-earth interface) is summarized. Chapter 3 contains the detailed analysis of the effects of the air-earth interface, and Chapter 4 is devoted to presentation of numerical examples and discussion of results.

CHAPTER 2

THE BURIED INSULATED CONDUCTOR (NEGLECTING THE AIR-EARTH INTERFACE)

The present section is a summary of the determination of the propagation constant for an infinitely long insulated wire buried in an infinite earth. Consider a cable of circular cross section imbedded in a conducting medium. The origin of coordinates is located at the center of the wire as shown in Figure 2-1. The center conductor is denoted medium (1) and has an outer radius a; the insulating layer, medium (2), has an outer radius b; and the earth, medium (3), extends to infinity.

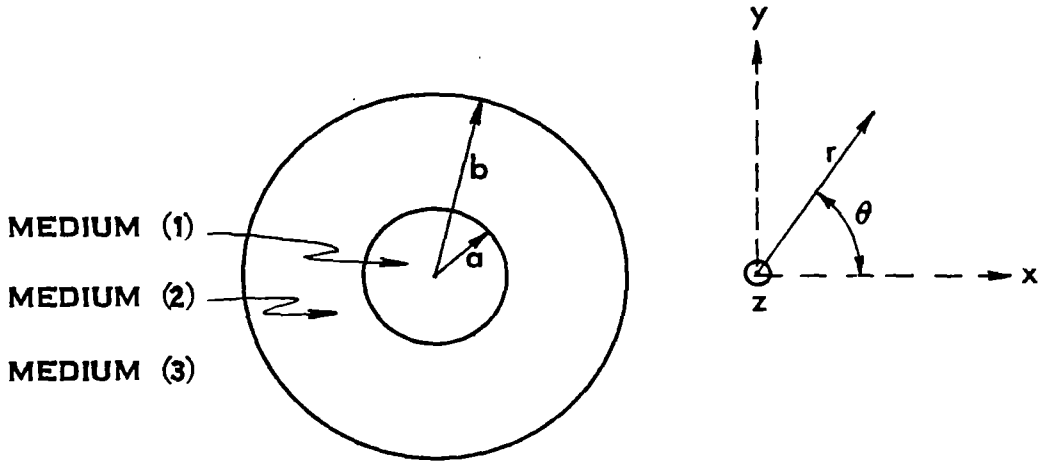

FIGURE 2-1

GEOMETRY OF INSULATED CABLE BURIED IN AN INFINITE MEDIUM

The determination of the propagation constant for this geometry has been discussed in detail by Ware, et al[1] who showed that the only mode of excitation of the cable that has small attenuation is the angularly symmetric Transverse Magnetic mode (the fundamental TM mode).

The remaining analysis is based upon a fundamental TM mode of excitation of the cable. The non-vanishing electric and magnetic fields in the jth medium can be written in terms of a single component Hertz vector[6]

$$E_z^{(j)} = \lambda_j^2 \Pi_z^{(j)} \tag{2-1}$$

$$E_r^{(j)} = ih \frac{\partial \Pi_z^{(j)}}{\partial r} = \frac{ih}{\lambda_j^2} \frac{\partial E_z^{(j)}}{\partial r} \tag{2-2}$$

$$H_\theta^{(j)} = \frac{ik_j^2}{\mu_j \omega} \frac{\partial \Pi_z^{(j)}}{\partial r} = \frac{ik_j^2}{\mu_j \omega \lambda_j^2} \frac{\partial E_z^{(j)}}{\partial r} \tag{2-3}$$

where

$$k_j^2 = \mu_j \omega (\epsilon_j \omega + i\sigma_j) \tag{2-4}$$

and

$$\lambda_j^2 = k_j^2 - h^2 \tag{2-5}$$

Standard notation is used: μ_j, ϵ_j, and σ_j are the permeability, permittivity and conductivity of the jth medium; and h is the propagation constant to be determined as a function of frequency.

Cylindrical symmetry allows the Hertz vectors to be expressed in terms of Bessel functions of order zero:

$$\Pi_z^{(1)} = A\, J_o(\lambda_1 r)\, e^{ihz-i\omega t} \qquad (0 \le r \le a) \qquad (2\text{-}6)$$

$$\Pi_z^{(2)} = [B\, J_o(\lambda_2 r) + C\, N_o(\lambda_2 r)] e^{ihz-i\omega t} \qquad (a \le r \le b) \qquad (2\text{-}7)$$

$$\Pi_z^{(3)} = D H_o^{(1)}(\lambda_3 r) e^{ihz-i\omega t} \qquad (b \le r \le \infty) \qquad (2\text{-}8)$$

The Hankel function of the first kind has been chosen to insure the fields behave like outgoing waves as $r \to \infty$. (We choose $Re\lambda > 0$).

The constant A, appearing in Equation (2-6) is related to the total current in the wire. The current density in the conductor is given by Ohm's Law, $J_z = \sigma_1 E_z^{(1)}$, and therefore the total current is

$$I = \int_o^a \int_o^{2\pi} \sigma_1 E_z^{(1)}\, r\, dr\, d\theta \qquad (2\text{-}9)$$

$$= 2\pi\sigma_1\, A\, e^{ihz-i\omega t} \int_o^a J_o(\lambda_1 r)\, r\, dr \qquad (2\text{-}10)$$

$$I = 2\pi a \sigma_1 \lambda_1 A J_1(\lambda_1 a)\, e^{ihz-i\omega t} \qquad (2\text{-}11)$$

The total current is sinusoidal with amplitude I_o,

$$I = I_o\, e^{ihz-i\omega t} \qquad (2\text{-}12)$$

hence

$$A = \frac{I_o}{2\pi a \sigma_1 \lambda_1 J_1(\lambda_1 a)} . \qquad (2\text{-}13)$$

The electric and magnetic fields in the center conductor are written

$$E_z^{(1)} = \frac{\lambda_1 I_o}{2\pi a \sigma_1} \cdot \frac{J_o(\lambda_1 r)}{J_1(\lambda_1 a)} e^{ihz-i\omega t} \tag{2-14}$$

$$E_r^{(1)} = \frac{-ihI_o}{2\pi a \sigma_1} \cdot \frac{J_1(\lambda_1 r)}{J_1(\lambda_1 a)} e^{ihz-i\omega t} \tag{2-15}$$

$$H_\theta^{(1)} = \frac{-ik_1^2 I_o}{2\pi a \sigma_1 \mu_1 \omega} \cdot \frac{J_1(\lambda_1 r)}{J_1(\lambda_1 a)} e^{ihz-i\omega t} \tag{2-16}$$

The fields in the insulator are

$$E_z^{(2)} = \lambda_2^2 [B\, J_o(\lambda_2 r) + C\, N_o(\lambda_2 r)]\, e^{ihz-i\omega t} \tag{2-17}$$

$$E_r^{(2)} = -ih\lambda_2 [B\, J_1(\lambda_2 r) + C\, N_1(\lambda_2 r)] e^{ihz-i\omega t} \tag{2-18}$$

$$H_\theta^{(2)} = \frac{-ik_2^2 \lambda_2}{\mu_2 \omega} [B\, J_1(\lambda_2 r) + C\, N_1(\lambda_2 r)]\, e^{ihz-i\omega t} \tag{2-19}$$

Finally, the fields in the earth are

$$E_z^{(3)} = \lambda_3^2\, D\, H_o^{(1)}(\lambda_3 r)\, e^{ihz-i\omega t} \tag{2-20}$$

$$E_r^{(3)} = -ih\lambda_3 D H_1^{(1)}(\lambda_3 r)\, e^{ihz-i\omega t} \tag{2-21}$$

$$H_\theta^{(3)} = \frac{-ik_3^2 \lambda_3}{\mu_3 \omega} D\, H_1^{(1)}(\lambda_3 r)\, e^{ihz-i\omega t}\,. \tag{2-22}$$

The determination of the remaining unknowns (B, C, D, and h) is made possible, in the usual fashion, by requiring the tangential components of the electric and magnetic fields to be continuous across the surfaces separating different materials. Application of these boundary conditions at r = a yields

$$\frac{\lambda_1 I_o}{2\pi a\sigma_1} \quad \frac{J_o(\lambda_1 a)}{J_1(\lambda_1 a)} = \lambda_2^2 \left[B\, J_o(\lambda_2 a) + C\, N_o(\lambda_2 a)\right] \qquad (2\text{-}23)$$

$$\frac{k_1^2 I_o}{2\pi a\sigma_1\mu_1} = \frac{k_2^2\lambda_2}{\mu_2} \left[B\, J_1(\lambda_2 a) + C\, N_1(\lambda_2 a)\right] \qquad (2\text{-}24)$$

Application of the boundary conditions at r = b yields

$$\lambda_2^2\left[B\, J_o(\lambda_2 b) + C\, N_o(\lambda_2 b)\right] = \lambda_3^2\, D\, H_o^{(1)}(\lambda_3 b) \qquad (2\text{-}25)$$

$$\frac{k_2^-\lambda_2}{\mu_2}\left[B\, J_1(\lambda_2 b) + C\, N_1(\lambda_2 b)\right] = \frac{k_3^-\lambda_3}{\mu_3}\, D\, H_1^{(1)}(\lambda_3 b). \qquad (2\text{-}26)$$

Equations (2-23) - (2-26) form a set of four simultaneous equations which may be solved for the four unknowns B, C, D, and h. However, all that is desired is the determination of the propagation constant h, so that Equation (2-25) may be divided by Equation (2-26) and the coefficient D eliminated at once. Similarly division of Equation (2-23) by Equation (2-24) reduces the coefficients B and C to their unknown ratio β = B/C. The simplest form of the result is the following two simultaneous equations in the two unknowns β and h.

$$\frac{\mu_1\lambda_1}{k_1^2} \cdot \frac{J_o(\lambda_1 a)}{J_1(\lambda_1 a)} = \frac{\mu_2\lambda_2}{k_2^2} \left[\frac{\beta\, J_o(\lambda_2 a) + N_o(\lambda_2 a)}{\beta\, J_1(\lambda_2 a) + N_1(\lambda_2 a)}\right] \qquad (2\text{-}27)$$

$$\frac{\mu_2\lambda_2}{k_2^2}\left[\frac{\beta\ J_o(\lambda_2 b)+ N_o(\lambda_2 b)}{\beta\ J_1(\lambda_2 b)+ N_1(\lambda_2 b)}\right] = \frac{\mu_3\lambda_3}{k_3^2}\cdot\frac{H_o^{(1)}(\lambda_3 b)}{H_1^{(1)}(\lambda_3 b)} \qquad (2\text{-}28)$$

It is worth repeating that Equations (2-27) and (2-28) are exact; no reference has been made to the specific properties of any medium, and no medium has been restricted in any manner.

A computer code[7] has been written to solve Equations (2-27) and (2-28) for the propagation constant h in the frequency range $0 \leq f \leq 10^8$ Hz. These results are shown in Figure 2-2. For some cases of practical interest, approximate analytical solutions for h can be obtained. Appendix A contains a low frequency ($f \lesssim 10^4$ Hz) solution for the case where medium (2) is a good insulator.

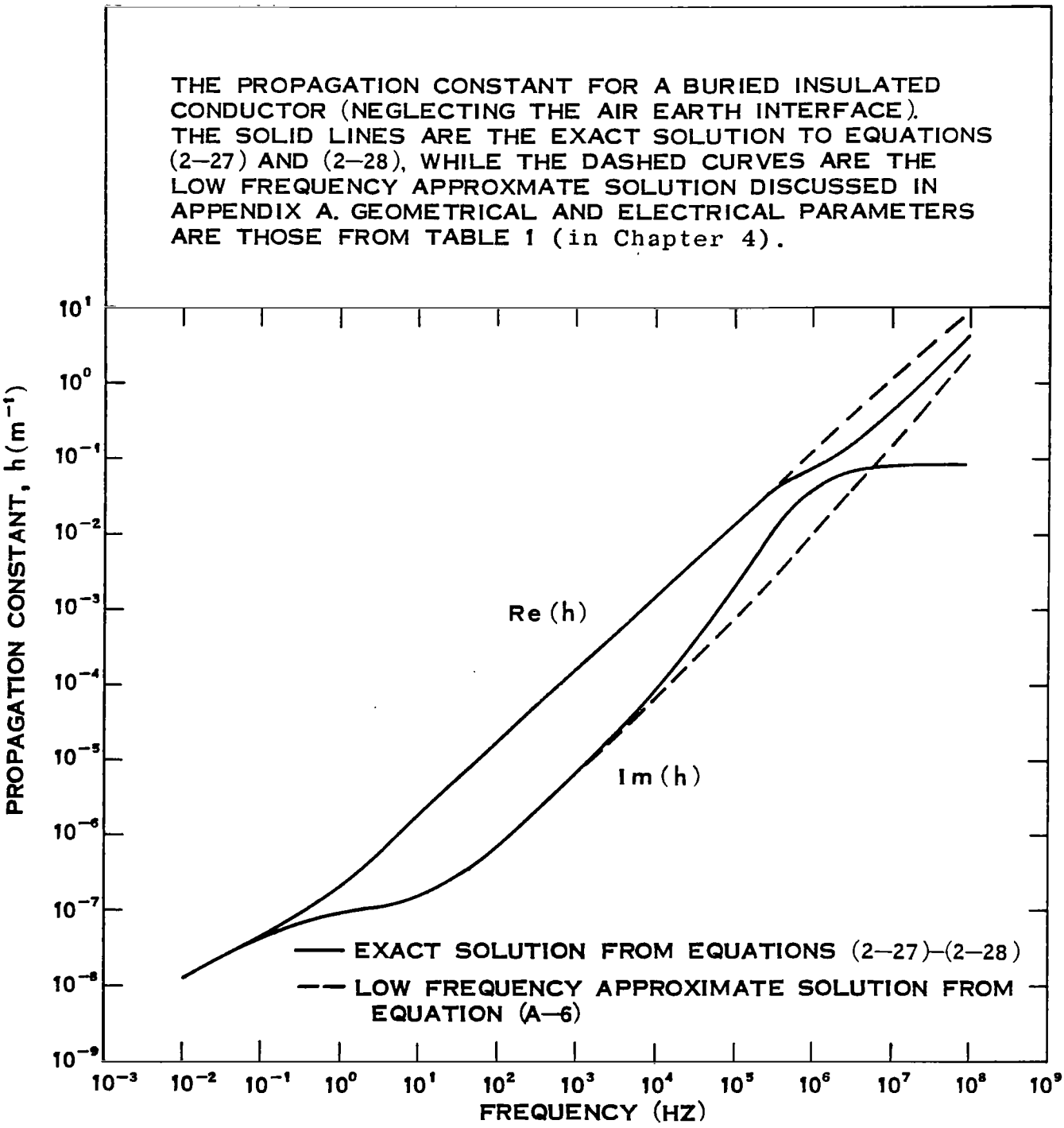

FIGURE 2—2

PROPAGATION CONSTANT FOR THE BURIED INSULATED CONDUCTOR (NEGLECTING REFLECTIONS FROM AIR—EARTH INTERFACE)

CHAPTER 3

THE EFFECT OF THE AIR-EARTH INTERFACE

The insulated conductor of the previous section is now placed at its proper position, a distance d below and parallel to a horizontal interface separating medium (3) and medium (4). the origin of coordinates is at the cable and the interface is defined as the plane y = d. The analysis is performed without identification of the physical characteristics of any of the four media.

The buried cable is of course a source of traveling electromagnetic waves. Consequently, the electric and magnetic fields in the neighborhood of the cable have two contributions: the primary fields of equations (2-20)-(2-22) and the secondary fields which arise from reflections from the air-ground interface. The resultant fields can be represented as the sum of these two components

$$\vec{E}^{TOTAL} = \vec{E}^{(3)} + \vec{E}^{REFLECTED} \qquad (3\text{-}1)$$

$$\vec{H}^{TOTAL} = \vec{H}^{(3)} + \vec{H}^{REFLECTED} \qquad (3\text{-}2)$$

It is these total fields to which the boundary conditions should be applied at the surface of the cable.

In general, the reflected fields do not have the cylindrical symmetry characteristic of the primary fields, however they can be decomposed into a symmetric part and a non-symmetric part. It is obvious that the non-symmetric part of the reflected fields can only excite non-symmetric modes in the cable which damp out quickly. Therefore it is only the cylindrically symmetric part of the reflected fields which contribute to the

fundamental TM excitation of the cable. For this part of the reflected fields, the boundary conditions at r = b can be satisfied without altering the form of the fields on the cable interior. Also observe that according to Equations (2-1)-(2-3), knowledge of E_z alone is sufficient to describe all the fundamental TM fields, so that only $E_z^{REFLECTED}$ need be evaluated.

As with any solution to the wave equation, the electric field of equations (2-1) and (2-2) can be constructed from plane wave solutions by the Fourier integral:

$$\vec{E}(x,y,z) \equiv \vec{E}(\vec{R}) = \int \vec{E}(\vec{k})\, e^{i\vec{k}\cdot\vec{R}}\, d\vec{k}. \qquad (3\text{-}3)$$

The Fourier amplitudes are obtained by inverting this expression to yield

$$\vec{E}(\vec{k}) = \frac{1}{(2\pi)^3} \int \vec{E}(\vec{R})\, e^{-i\vec{k}\cdot\vec{R}}\, d\vec{R}. \qquad (3\text{-}4)$$

Thus, the scattering of the primary fields is reduced in the usual manner to the scattering of plane waves.

The scattering of a single plane wave is depicted in Figure 3-1 where $\vec{k}_o$, $\vec{k}_R$, and $\vec{k}_T$ are the wave vectors for the incident, reflected and transmitted waves respectively, and $\hat{n}$ is a unit vector normal to the interface.

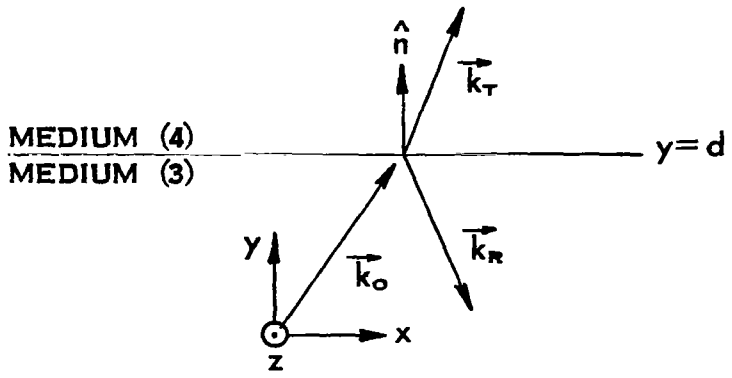

FIGURE 3-1

For a source located at the origin, the fields are written

$$\vec{E}_o = \vec{E}_o e^{i\vec{k}_o \cdot \vec{R}} \tag{3-5}$$

$$\vec{E}_R = \vec{E}_R e^{i\vec{k}_R \cdot \vec{R} + i\Phi_R} \tag{3-6}$$

$$\vec{E}_T = \vec{E}_T e^{i\vec{k}_T \cdot \vec{R} + i\Phi_T} \tag{3-7}$$

and of course,

$$|\vec{k}_o|^2 = |\vec{k}_R|^2 = k_3^2 = \mu_3\omega(\epsilon_3\omega + i\sigma_3) \tag{3-8}$$

$$|\vec{k}_T|^2 = k_4^2 = \mu_4\omega\,(\epsilon_4\omega + i\sigma_4) \tag{3-9}$$

The problem is to determine the amplitudes $\vec{E}_R$ and $\vec{E}_T$ in terms of $\vec{E}_o$ with the aid of boundary conditions at the surface y=d.

A necessary condition for the boundary conditions to be fulfilled is that the phases of all three waves be identical at the interface.

$$k_{o_x} x + k_{o_y} d + k_{o_z} z$$

$$= k_{R_x} x + k_{R_y} d + k_{R_z} z + \Phi_R \qquad (3\text{-}10)$$

$$= k_{T_x} x + k_{T_y} d + k_{T_z} z + \Phi_T$$

Since these relations must be maintained for all values of x and z, k_x and k_z are invariants of the scattering,

$$k_{o_x} = k_{R_x} = k_{T_x} \qquad (3\text{-}11)$$

$$k_{o_z} = k_{R_z} = k_{T_z} \qquad (3\text{-}12)$$

By virtue of equations (3-8) and (3-9), and Figure 3-1, it is apparent that

$$k_{R_y} = -k_{o_y} \qquad (3\text{-}13)$$

$$k_{T_y} = \sqrt{k_4^2 - k_3^2 + k_{o_y}^2} \qquad (3\text{-}14)$$

The relations (3-11) - (3-14) are readily identified as Snell's Laws, which allow the phase factors to be written explicitly as

$$\Phi_R = 2 k_{o_y} d \qquad (3\text{-}15)$$

$$\Phi_T = (k_{o_y} - k_{T_y}) d. \qquad (3\text{-}16)$$

The field amplitudes are

$$\vec{E}_o = \vec{E}_o \exp\{i(k_{o_x} x + k_{o_y} y + k_{o_z} z)\} \quad (3\text{-}17)$$

$$\vec{E}_R = \vec{E}_R \exp\{i(k_{o_x} x + k_{o_y} (2d-y) + k_{o_z} z)\} \quad (3\text{-}18)$$

$$\vec{E}_T = \vec{E}_T \exp\{i(k_{o_x} x + k_{T_y} (y-d) + k_{o_z} z + k_{o_y} d)\}. \quad (3\text{-}19)$$

The incident plane wave $\vec{E}_o$ is in the general case, neither perpendicular nor parallel to the plane of incidence (the plane defined by $\hat{n}$ and $\vec{k}_o$). It is therefore convenient to define a new coordinate system whose unit vectors are given relative to the wave vector $\vec{k}_j$ for each wave $\vec{E}_j$ (j = 0, R, T):

$$\hat{n}_k^{(j)} = \frac{k_j}{|\vec{k}_j|} = \frac{k_{o_x} \hat{x} + k_{j_y} \hat{y} + k_{o_z} \hat{z}}{k_j} \quad (3\text{-}20)$$

$$\hat{n}_\perp^{(j)} = \frac{\hat{n} \times \vec{k}_j}{|\hat{n} \times \vec{k}_j|} = \frac{k_{o_z} \hat{x} - k_{o_x} \hat{z}}{\sqrt{k_{o_x}^2 + k_{o_z}^2}} \quad (3\text{-}21)$$

$$\hat{n}_\parallel^{(j)} = \frac{\hat{n}_\perp^{(j)} \times \vec{k}_j}{|\hat{n}_\perp^{(j)} \times \vec{k}_j|} = \frac{k_{o_x} k_{j_y} \hat{x} - (k_{o_x}^2 + k_{o_z}^2) \hat{y} + k_{j_y} k_{o_z} \hat{z}}{k_j \sqrt{k_{o_x}^2 + k_{o_z}^2}} \quad (3\text{-}22)$$

$\hat{n}_\perp^{(j)}$ is normal to the plane of incidence, $\hat{n}_\parallel^{(j)}$ is in the plane of incidence, and both are transverse to $\vec{k}_j$, as shown in Figure 3-2.

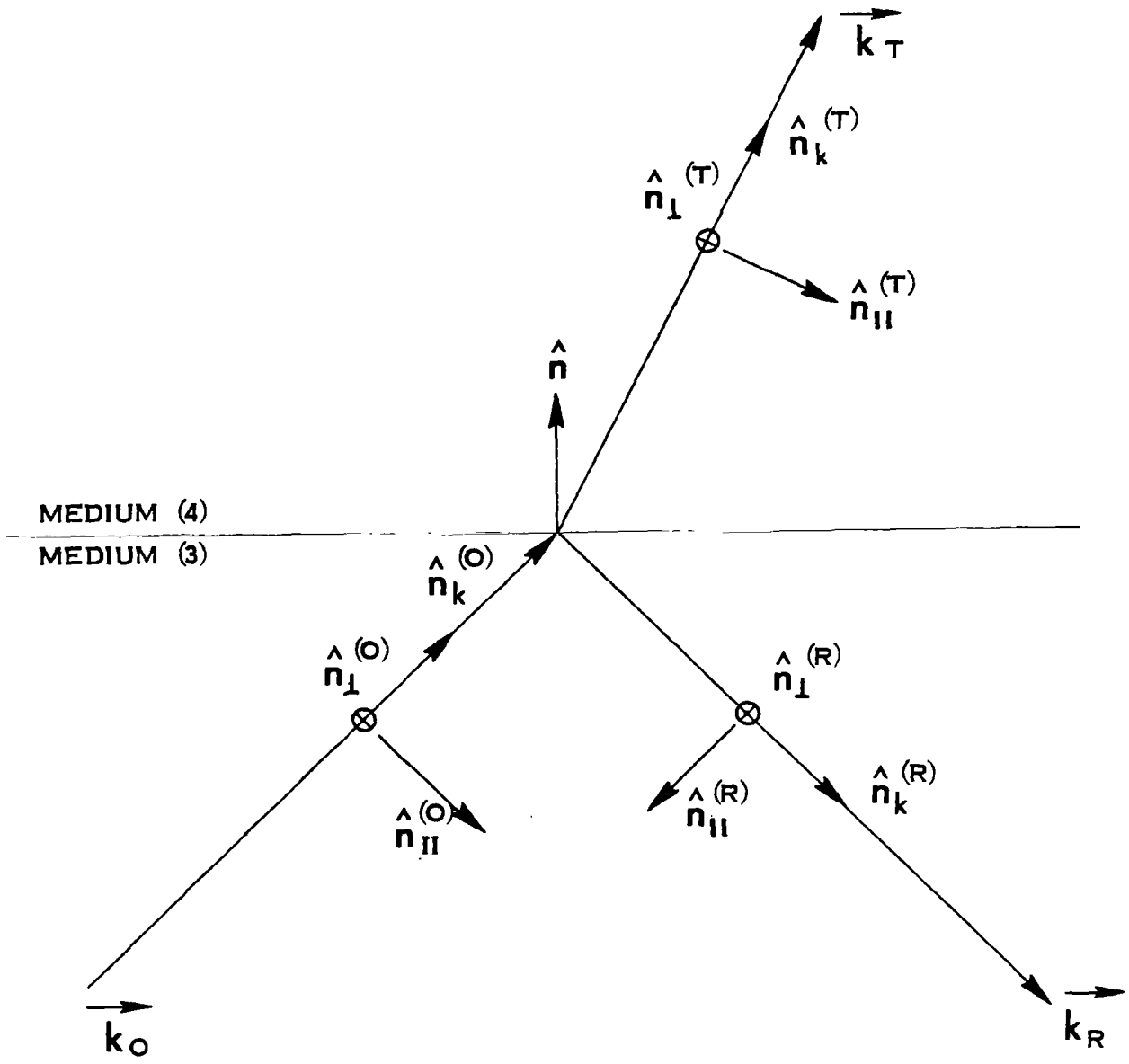

FIGURE 3-2

THE RELATIVE ORIENTATION OF THE BASIS VECTORS

Since $\vec{E}_j$ is always transverse to $\vec{k}_j$, it can be represented by components along $\hat{n}_\perp^{(j)}$ and $\hat{n}_\parallel^{(j)}$

$$\vec{E}_o = E_{o_\perp} \hat{n}_\perp^{(o)} + E_{o_\parallel} \hat{n}_\parallel^{(o)} \quad . \tag{3-23}$$

And since $\vec{E}_o$ is known, its polarization components can be found by

$$E_{o_\perp} = \vec{E}_o \cdot \hat{n}_\perp^{(o)} \tag{3-24}$$

$$E_{o_\parallel} = \vec{E}_o \cdot \hat{n}_\parallel^{(o)} \tag{3-25}$$

These polarization components transform according to the standard Fresnel coefficients $f_{R_\perp}$, $f_{R_\parallel}$, $f_{T_\perp}$, $f_{T_\parallel}$ (Appendix B), so that

$$\vec{E}_R = (f_{R_\perp} E_{o_\perp}) \hat{n}_\perp^{(R)} + (f_{R_\parallel} E_{o_\parallel}) \hat{n}_\parallel^{(R)} \tag{3-26}$$

$$\vec{E}_T = (f_{T_\perp} E_{o_\perp}) \hat{n}_\perp^{(T)} + (f_{T_\parallel} E_{o_\parallel}) \hat{n}_\parallel^{(T)} \tag{3-27}$$

where

$$f_{R_\parallel} = \frac{k_4^2 \mu_3 k_{o_y} - k_3^2 \mu_4 k_{T_y}}{k_4^2 \mu_3 k_{o_y} + k_3^2 \mu_4 k_{T_y}} \tag{3-28}$$

$$f_{R_\perp} = \frac{\mu_4 k_{o_y} - \mu_3 k_{T_y}}{\mu_4 k_o + \mu_3 k_T} \tag{3-29}$$

$$f_{T_{\parallel}} = \left(\frac{k_4\mu_3}{k_3\mu_4}\right) \cdot \frac{2k_4^2\mu_3 k_{o_y}}{k_4^2\mu_3 k_{o_y} + k_3^2\mu_4 k_{T_y}} \tag{3-30}$$

$$f_{T_{\perp}} = \frac{2\mu_4 k_{o_y}}{\mu_4 k_{o_y} + \mu_3 k_{T_y}} \quad . \tag{3-31}$$

The reflected field is expressed in cartesian coordinates by virtue of definitions (3-21) and (3-22), e.g.,

$$E_{R_z} = f_{R_{\perp}}(\vec{E}_o \cdot \hat{n}_{\perp}^{(o)})\left(\frac{-k_{o_x}}{\sqrt{k_{o_x}^2 + k_{o_z}^2}}\right)$$

$$+ f_{R_{\parallel}}(\vec{E}_o \cdot \hat{n}_{\parallel}^{(o)})\left(\frac{-k_{o_y} k_{o_z}}{k_3\sqrt{k_{o_x}^2 + k_{o_z}^2}}\right) \quad , \tag{3-32}$$

The primary field of Equation (2-20) may be transformed into cartesian coordinates by the integral[8]

$$H_o^{(1)}(\lambda r) = \frac{1}{\pi} \int_{-\infty}^{\infty} e^{i\xi x + iy\sqrt{\lambda^2-\xi^2}} \frac{d\xi}{\sqrt{\lambda^2-\xi^2}} \quad , \tag{3-33}$$

where the variable of integration is real even though λ may be complex. With this representation for the Hankel function, the primary electric field is

$$E_z^{(3)}(x,y,z) = \frac{D}{\pi} \lambda_3^2 \, e^{ihz - i\omega t} \int_{-\infty}^{\infty} e^{i\xi x + iy\sqrt{\lambda_3^2-\xi^2}} \frac{d\xi}{\sqrt{\lambda_3^2-\xi^2}} \quad . \tag{3-34}$$

The Fourier coefficient for E_z can be written down by comparison of Equations (3-3) and (3-34) (identify ξ with k_{o_x})

$$E_{o_z}(\vec{k}_o) = \frac{D}{\pi} \lambda_3^2 \frac{1}{\sqrt{\lambda_3^2 - \xi^2}} \delta\left(k_{o_y} - \sqrt{\lambda_3^2 - \xi^2}\right) \delta\left(k_{o_z} - h\right) \qquad (3\text{-}35)$$

The x and y- components of $\vec{E}_o$ can be derived from E_{o_z} by means of the Hertz vector,

$$E_x^{(3)}(x,y,z) = ih \frac{\partial \Pi_z^{(3)}}{\partial x} \; ; \; E_y^{(3)}(x,y,z) = ih \frac{\partial \Pi_z^{(3)}}{\partial y} \qquad (3\text{-}36)$$

However these derivatives may be taken under the Fourier integral to obtain

$$E_{o_x}(\vec{k}_o) = - \frac{\xi h}{\lambda_3^2} E_{o_z}(\vec{k}_o) \qquad (3\text{-}37)$$

$$E_{o_y}(\vec{k}_o) = - \frac{k_{o_y} h}{\lambda_3^2} E_{o_z}(\vec{k}_o) \qquad (3\text{-}38)$$

Thus

$$\vec{E}_o(\vec{k}_o) = E_{o_z}(\vec{k}_o) \left\{ - \frac{k_{o_x} k_{o_z}}{\lambda_3^2} \hat{x} - \frac{k_{o_y} k_{o_z}}{\lambda_3^2} \hat{y} + \hat{z} \right\}, \qquad (3\text{-}39)$$

whose polarization components are

$$E_{o_\perp} = - E_{o_z} \left(\frac{k_{o_x} k_3^2}{\lambda_3^2 \sqrt{k_{o_x}^2 + k_{o_z}^2}} \right) \qquad (3\text{-}40)$$

and

$$E_{o_\parallel} = E_{o_z} \left(\frac{k_3 k_{o_y} k_{o_z}}{\lambda_3^2 \sqrt{k_{o_x}^2 + k_{o_z}^2}} \right) . \qquad (3\text{-}41)$$

The complete, reflected z-component electric field is then found to be

$$E_z^R(x,y,z) = \frac{D}{\pi} e^{ihz-i\omega t} \int_{-\infty}^{\infty} e^{i\left[\xi x+(2d-y)\sqrt{\lambda_3^2-\xi^2}\right]} \left\{ k_3^2 \xi^2 f_{R_\perp} - h^2(\lambda_3^2-\xi^2) f_{R_{||}} \right\} \frac{d\xi}{(\xi^2+h^2)\sqrt{\lambda_3^2-\xi^2}} \quad (3\text{-}42)$$

Of this result for the reflected field, only the cylindrically symmetric portion is desired.

Any plane wave can be expanded into cylindrical waves according to

$$e^{i(k_x x + k_y y)} = \sum_{n=-\infty}^{\infty} (i)^n J_n(\lambda r) e^{in\theta} \quad (3\text{-}43)$$

where $\lambda = \sqrt{k_x^2 + k_y^2}$ and θ is the angle between $\vec{\lambda}$ and $\vec{r}$. Thus the cylindrically symmetric portion of the reflected field is formed entirely from the n=0 term in the expansion.

$$E_z^{\text{REFLECTED}}(r,z) = D\, e^{ihz-i\omega t} J_o(\lambda_3 r) F(k_3, k_4, h, d), \quad (3\text{-}44)$$

where

$$F(k_3,k_4,h,d) \equiv \frac{1}{\pi} \int_{-\infty}^{\infty} e^{i2d\sqrt{k_3^2-h^2-\xi^2}} \left\{ k_3^2 \xi^2 f_{R_\perp} - h^2(k_3^2-h^2-\xi^2) f_{R_{||}} \right\} \frac{d\xi}{(\xi^2+h^2)\sqrt{k_3^2-h^2-\xi^2}} \quad (3\text{-}45)$$

with

$$f_{R_\perp} = \frac{\mu_4\sqrt{k_3^2-h^2-\xi^2} - \mu_3\sqrt{k_4^2-h^2-\xi^2}}{\mu_4\sqrt{k_3^2-h^2-\xi^2} + \mu_3\sqrt{k_4^2-h^2-\xi^2}} \tag{3-46}$$

and

$$f_{R_{||}} = \frac{\mu_3 k_4^2\sqrt{k_3^2-h^2-\xi^2} - \mu_4 k_3^2\sqrt{k_4^2-h^2-\xi^2}}{\mu_3 k_4^2\sqrt{k_3^2-h^2-\xi^2} + \mu_4 k_3^2\sqrt{k_4^2-h^2-\xi^2}} \tag{3-47}$$

Consequently by virtue of relation (2-3), the cylindrically symmetric reflected magnetic field is

$$H_\theta^{REFLECTED}(r,z) = -\frac{Dik_3^2}{\mu_3\omega\lambda_3} e^{ihz-i\omega t} J_1(\lambda_3 r)F(k_3,k_4,h,d). \tag{3-48}$$

The addition of the reflected fields to the primary fields provides a new set of fields which must satisfy boundary conditions on the cable's surface. The simultaneous equations are handled in exactly the same manner as in the previous section, resulting in the following equations to be solved for the propagation constant.

$$\frac{\mu_1\lambda_1}{k_1^2}\cdot\frac{J_o(\lambda_1 a)}{J_1(\lambda_1 a)} = \frac{\mu_2\lambda_2}{k_2^2}\left[\frac{\beta J_o(\lambda_2 a) + N_o(\lambda_2 a)}{\beta J_1(\lambda_2 a) + N_1(\lambda_2 a)}\right] \tag{2-27}$$

$$\frac{\mu_2\lambda_2}{k_2^2}\left[\frac{\beta J_o(\lambda_2 b) + N_o(\lambda_2 b)}{\beta J_1(\lambda_2 b) + N_1(\lambda_2 b)}\right]$$

$$= \frac{\mu_3\lambda_3}{k_3^2}\left[\frac{H_o^{(1)}(\lambda_3 b)+J_o(\lambda_3 b)\cdot F(k_3,k_4,h,d)/\lambda_3^2}{H_1^{(1)}(\lambda_3 b)+J_1(\lambda_3 b)\cdot F(k_3,k_4,h,d)/\lambda_3^2}\right] \tag{3-49}$$

The net effect of the air-earth interface is to introduce a modification to the right hand side of Equation (2-28).

CHAPTER 4

NUMERICAL EXAMPLES

Numerical values of the electrical and geometrical parameters of the buried insulated cable are contained in Table 1. Unless otherwise specified all the calculations of the present chapter are based on these values.

The integral appearing in Equation (3-45) can, under certain approximations, be treated analytically[3], however no attempt has been made to do so. A computer subprogram has been written to evaluate this integral numerically using a simple Simpson's Rule technique. The value of the integral F was then used in the simultaneous solution of Equations (2-27) and (3-49) for h. Before presenting these propagation constants, insight into the problem is developed through some intermediate results.

Figure 4-1 shows the reflection coefficient at normal incidence for the frequency range 10^{-2} Hz $\leq f \leq 10^{8}$ Hz. (Note that at normal incidence, $f_{R_\perp} \equiv f_{R_\parallel}$). The frequency range from $\sim 10^{4}$ Hz to $\sim 10^{7}$ Hz is shown to be most interesting since it is in this region that the soil makes the transition from "good conductor" to "good insulator." Figure 4-2 shows the variation of the reflection coefficients as evaluated at different values of ξ from the integration of Equation (3-45) at the arbitrary frequency of 10^{5} Hz. Similarly the entire integrand of Equation (3-45) is shown as a function of ξ in Figure 4-3. These figures are presented without much comment since they are included only to give the reader some feeling for the numerical integration.

TABLE 1

ELECTRICAL AND GEOMETRICAL PARAMETERS USED IN THE NUMERICAL EXAMPLES

j	MEDIUM	CONDUCTIVITY (mho/m)	PERMITTIVITY ($\epsilon_o = 8.854 \times 10^{-12}$ farad/m)	PERMEABILITY ($\mu_o = 4\pi \times 10^{-7}$ henry/m)
1	conductor (copper)	5.8×10^7	ϵ_o	μ_o
2	Insulator	0	$4\,\epsilon_o$	μ_o
3	Earth	10^{-3}	$4\,\epsilon_o$	μ_o
4	Air	0	ϵ_o	μ_o

radius of central conductor, a = 0.01794 m

outer radius of insulator, b = 0.03588 m

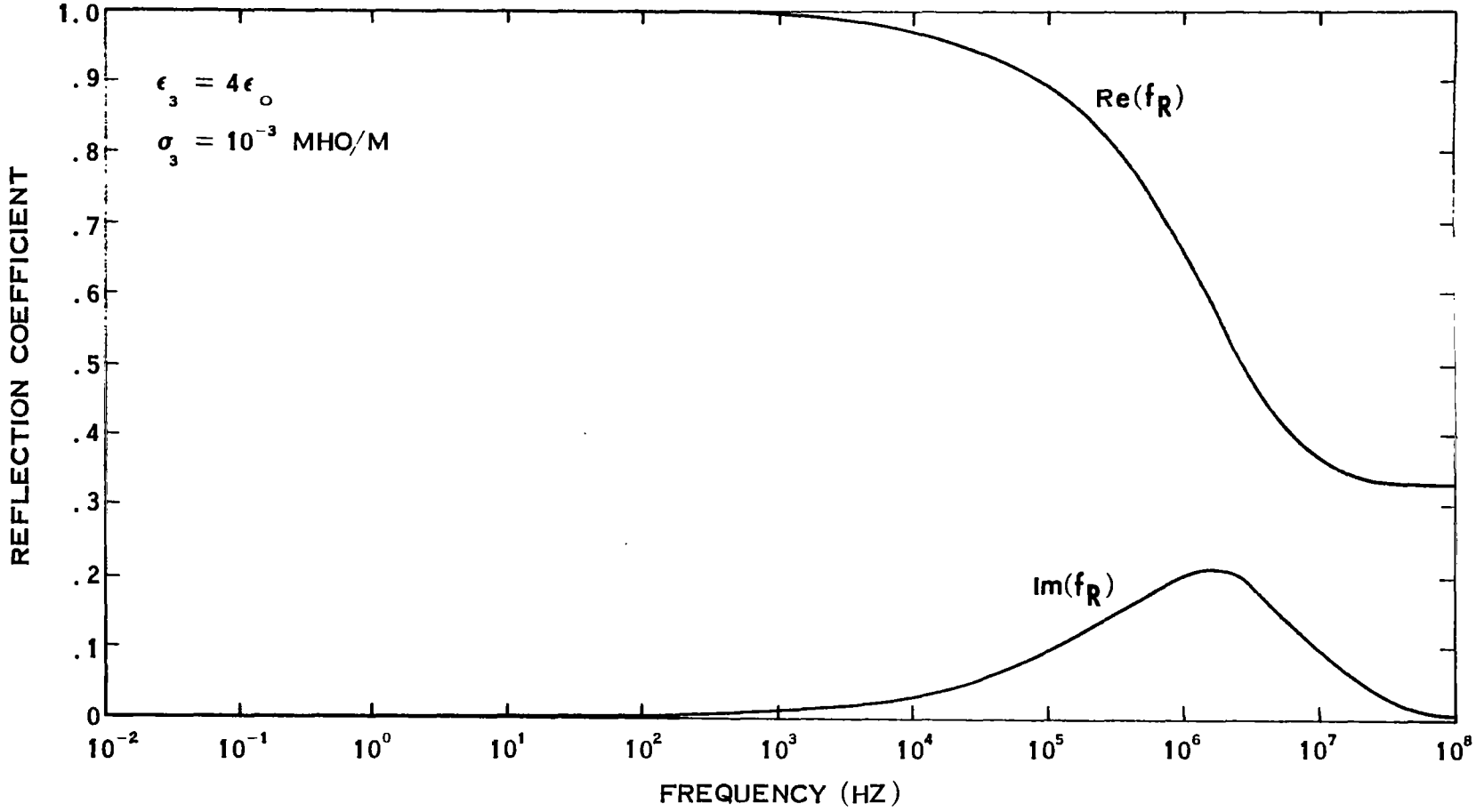

FIGURE 4–1

REFLECTION COEFFICIENT AT NORMAL INCIDENCE

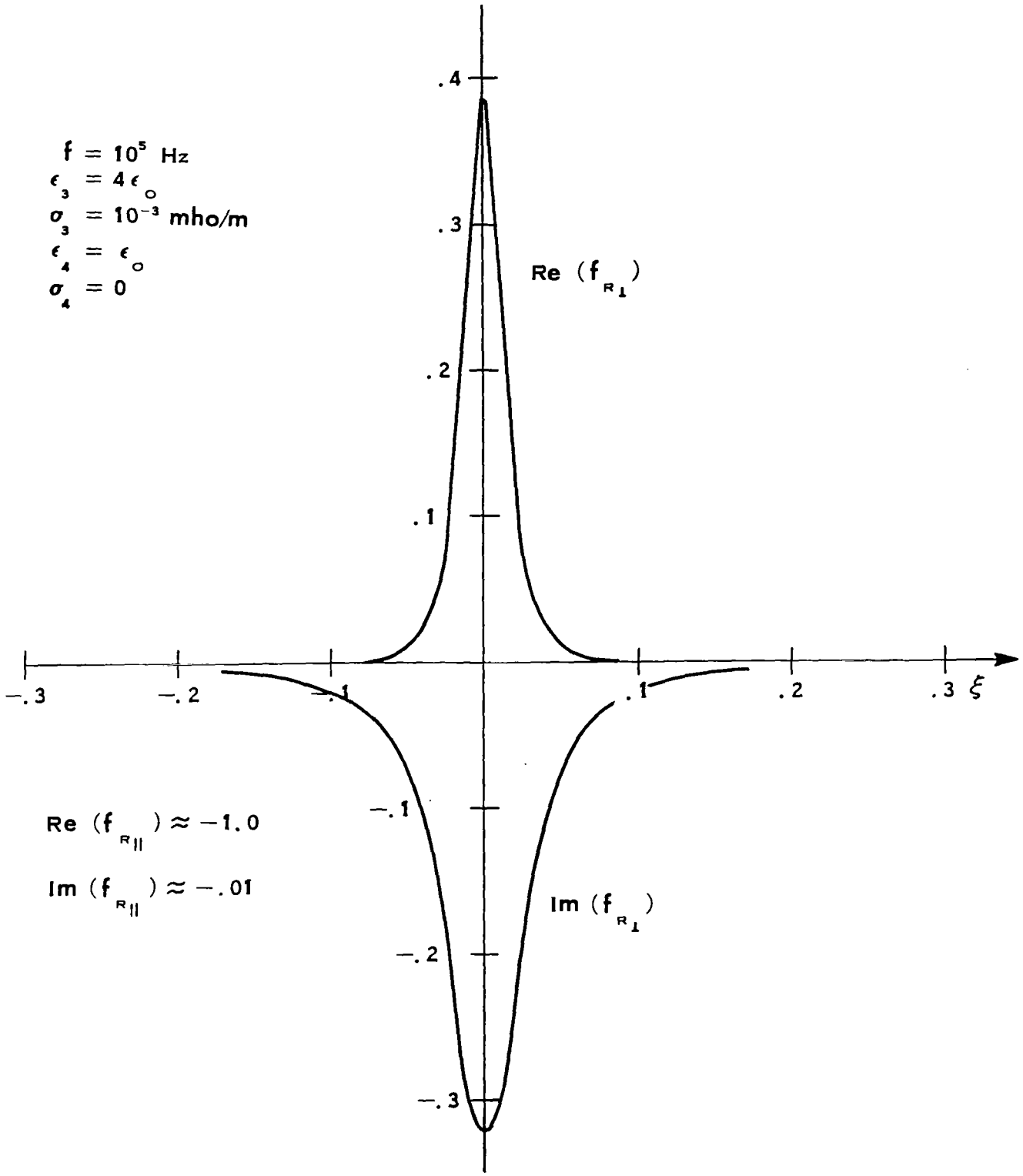

FIGURE 4−2

REFLECTION COEFFICIENTS

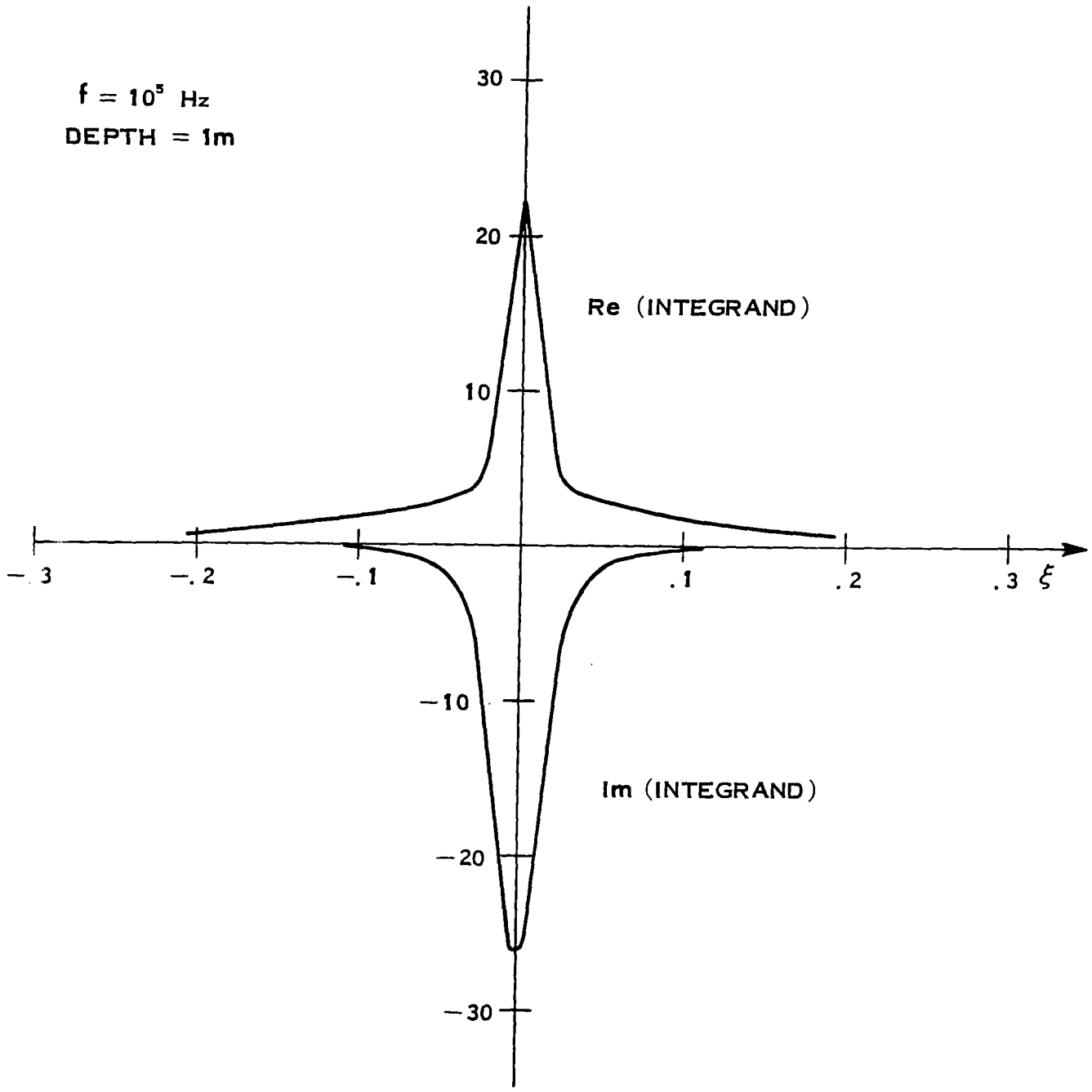

FIGURE 4−3

THE INTEGRAND OF EQUATION (3−45)

In the final analysis, any change in the propagation constant must be the result of a change in the electromagnetic fields near the cable (E_z and H_θ). Figures 4-4 and 4-5 show the relative magnitude of the reflected fields (TM components only) at the cable surface for a burial depth of 100 m. The reflected azimuthal magnetic field, $H_\theta^{REFLECTED}$, is never more than $\sim 10^{-8}$ of the primary azimuthal magnetic field, $H_\theta^{(3)}$, and could probably have been neglected throughout. On the other hand, the reflected longitudinal electric field $E_z^{REFLECTED}$ makes up a significant portion of the total field near the cable. Physically, the electromagnetic environment near the cable has been altered by the presence of the air-earth interface through the large reflected longitudinal electric field. Finally, the correction factor F/λ_3^2 which makes Equation (3-49) different from Equation (2-28) is plotted as a function of frequency in Figure 4-6 (again at a burial depth of 100 m).

The propagation constant h has been determined from Equations (2-27) and (3-49) for burial depths of 1 m, 10 m, 100 m, and 1000 m. These are presented in Figures 4-7 through Figure 4-10 as the fractional change in h relative to h_∞, the "infinite burial depth" result of Chapter 2. The results will be discussed shortly.

Recently it has been determined by measurement that the soil parameters of Table 1 are less realistic than the frequency dependent parameters:

$$\epsilon_3 = 3\times10^{6}\ f^{-0.78}\ \epsilon_o$$

$$\sigma_3 = \left\{ \begin{array}{ll} 8\times10^{-5}\ f^{2/3} & \text{mho/m for } f \le 10^{3} \text{ Hz} \\ 5.3\times10^{-3} & \text{mho/m for } f \ge 10^{3} \text{ Hz} \end{array} \right\} . \qquad (4\text{-}1)$$

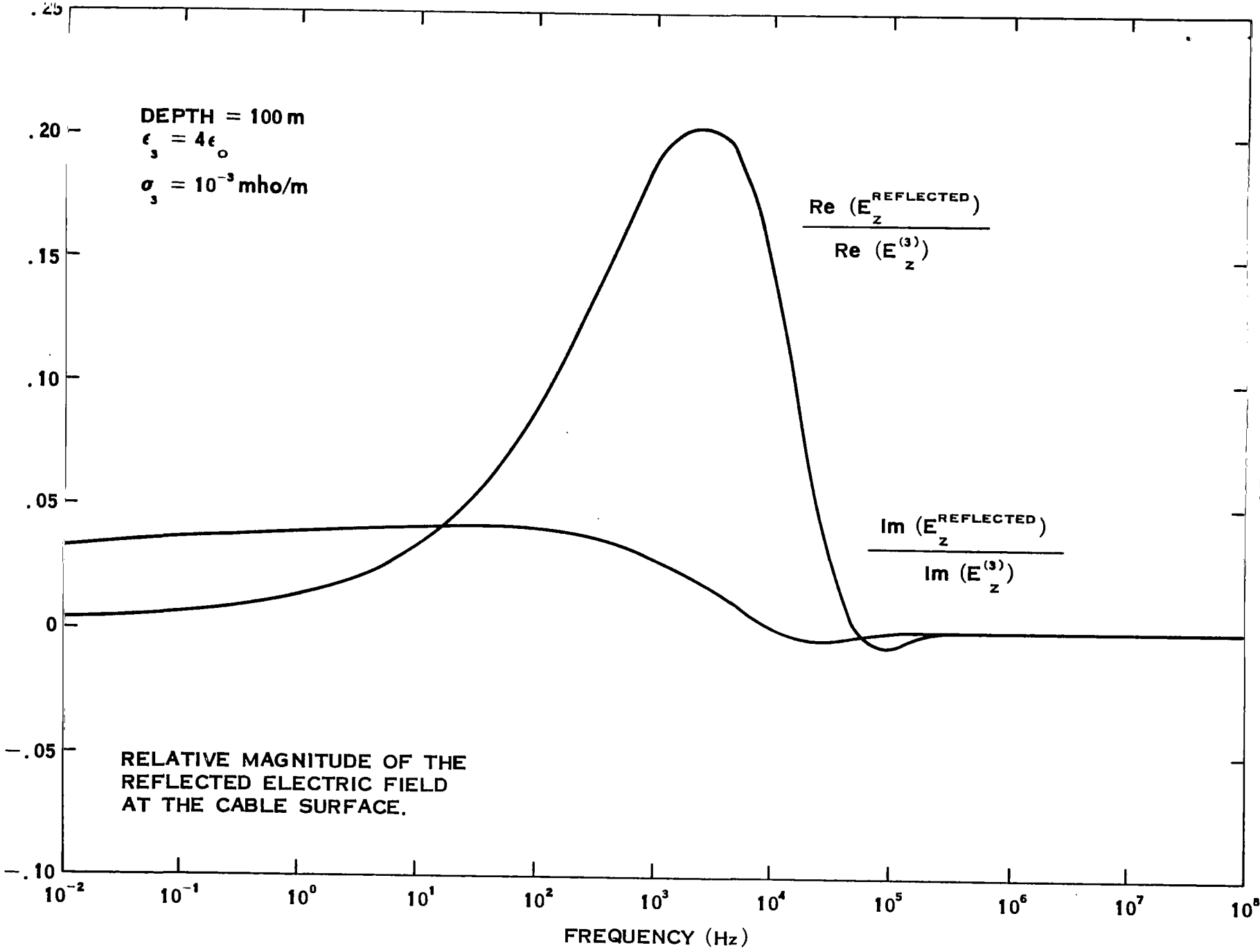
DEPTH = 100 m
$\epsilon_3 = 4\epsilon_o$
$\sigma_3 = 10^{-3}$ mho/m
$\frac{\text{Re } (E_z^{\text{REFLECTED}})}{\text{Re } (E_z^{(3)})}$
$\frac{\text{Im } (E_z^{\text{REFLECTED}})}{\text{Im } (E_z^{(3)})}$
RELATIVE MAGNITUDE OF THE REFLECTED ELECTRIC FIELD AT THE CABLE SURFACE.
.25
.20
.15
.10
.05
0
−.05
−.10
10^{-2}
10^{-1}
10^{0}
10^{1}
10^{2}
10^{3}
10^{4}
10^{5}
10^{6}
10^{7}
10^{8}
FREQUENCY (Hz)

FIGURE 4−4

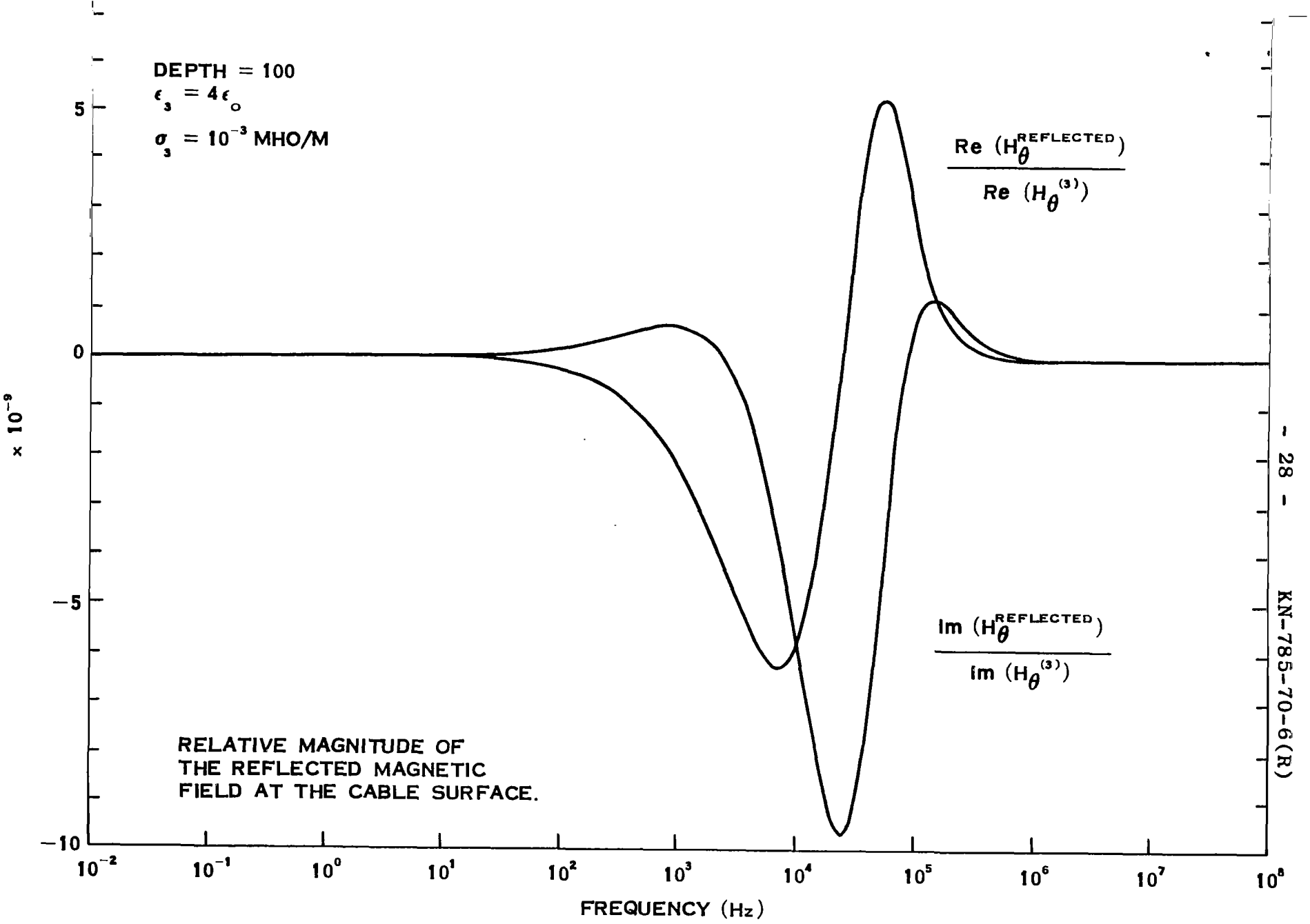

FIGURE 4−5

KN-785-70-6(R)

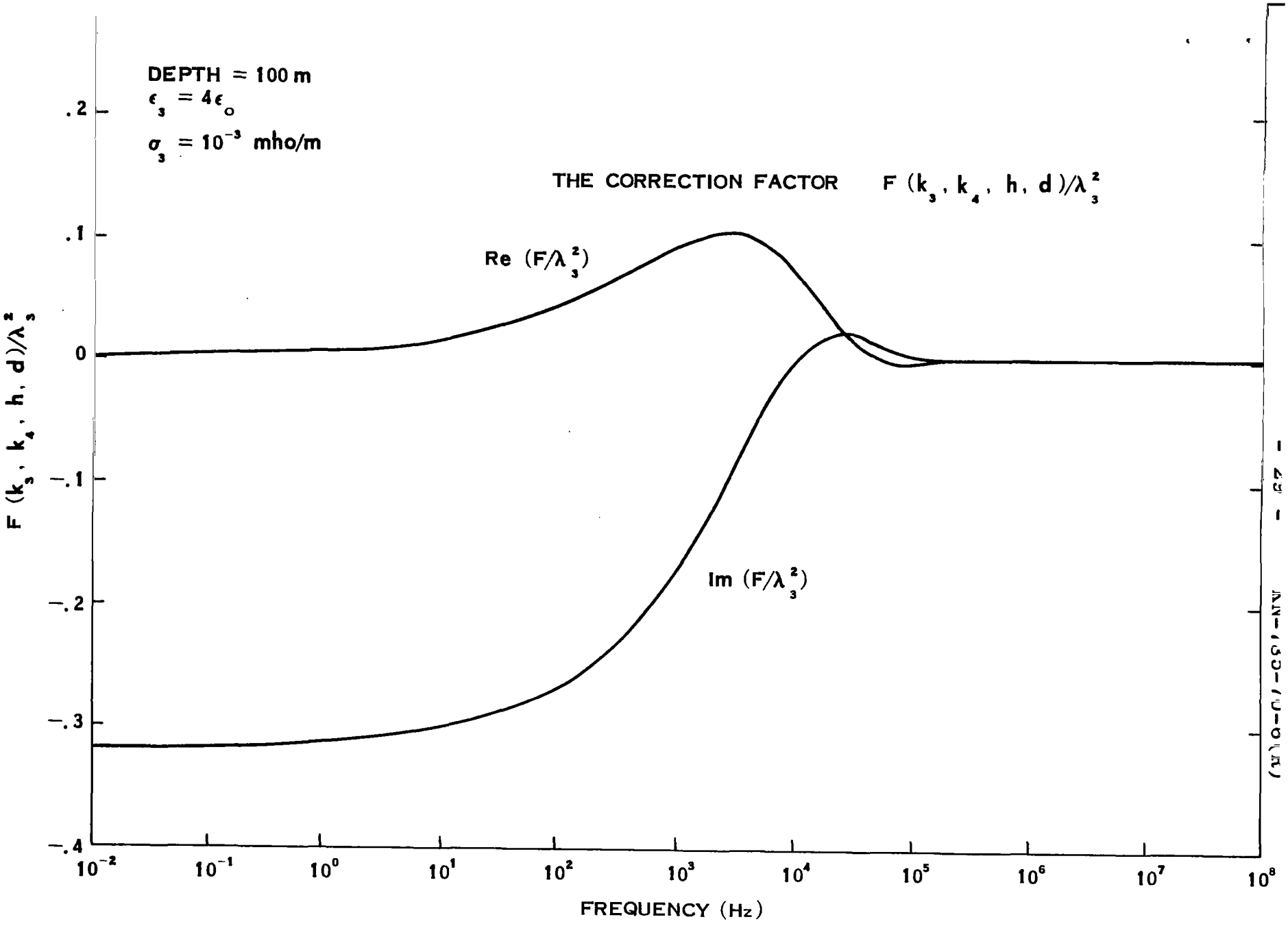

FIGURE 4−6

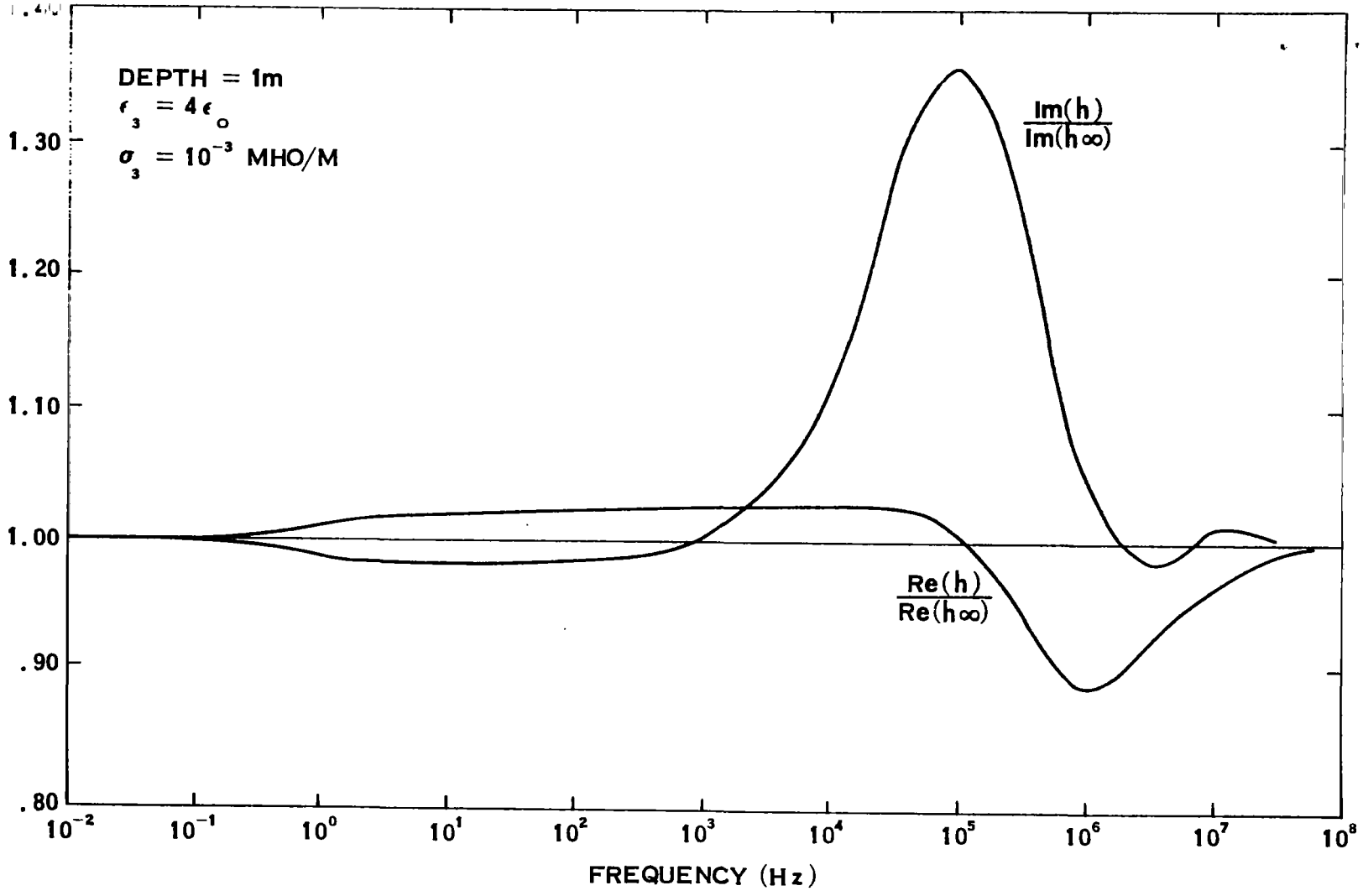

FIGURE 4-7

FRACTIONAL CHANGE IN THE PROPAGATION CONSTANT

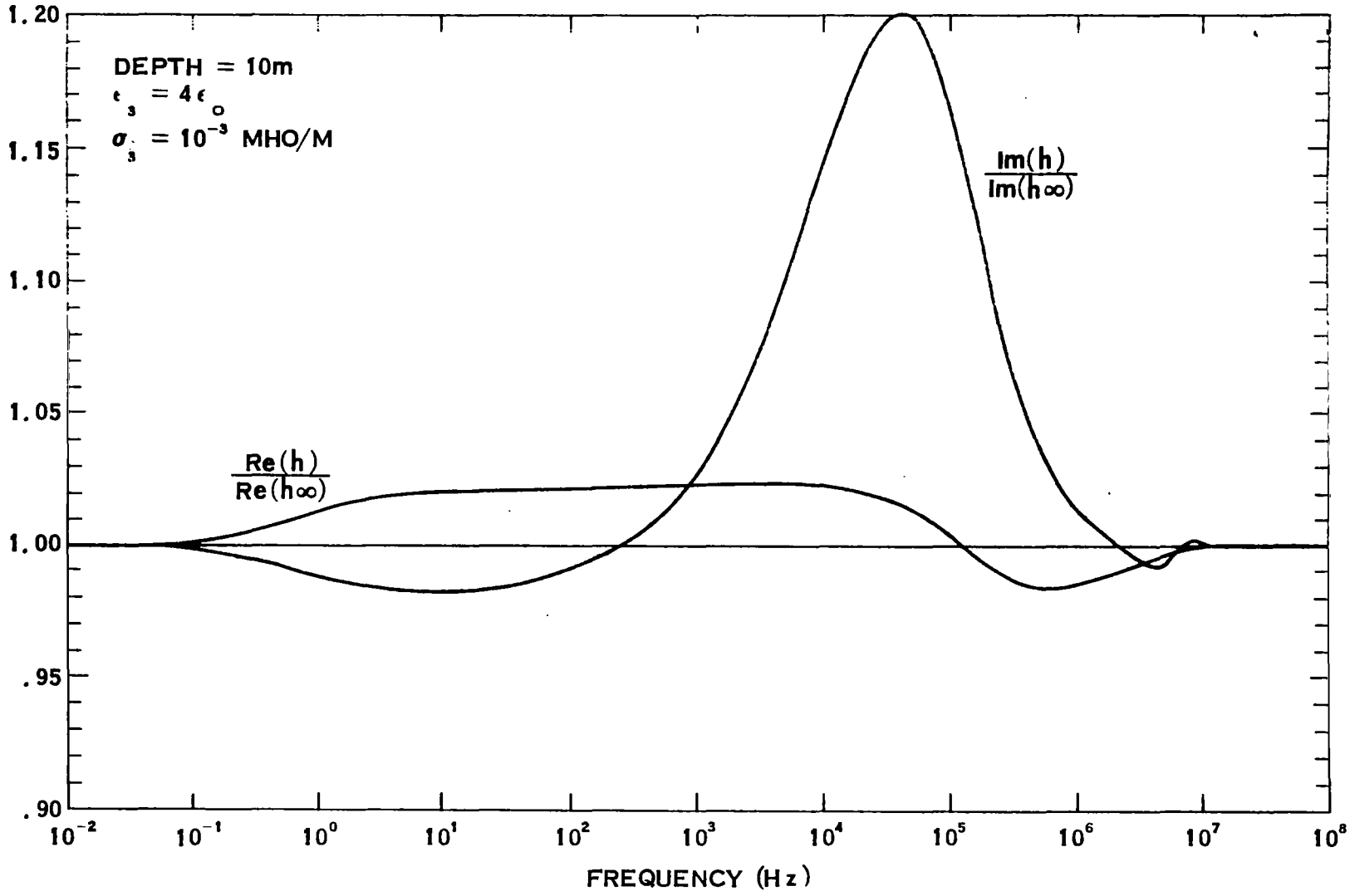

FIGURE 4-8

FRACTIONAL CHANGE IN THE PROPAGATION CONSTANT

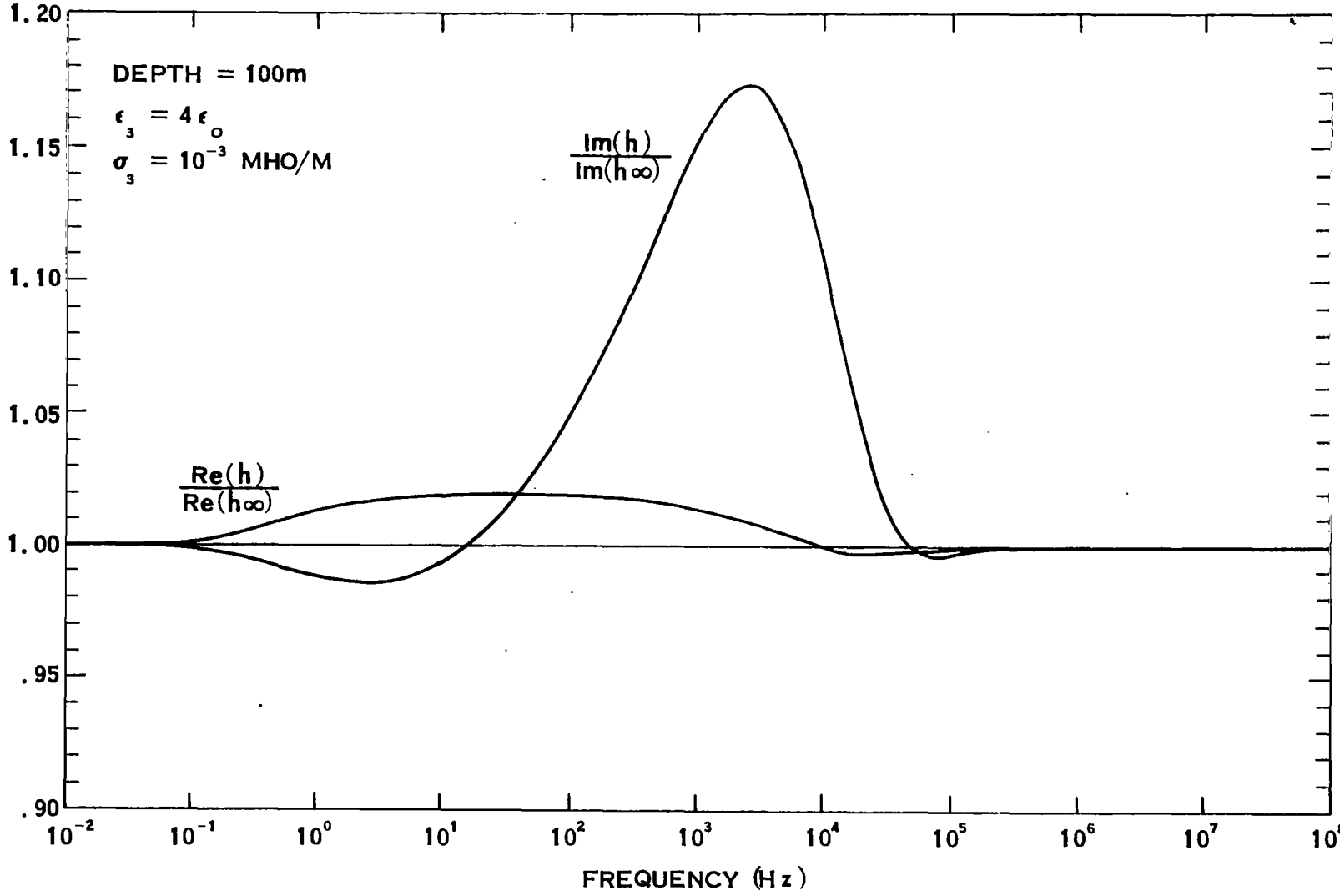

FIGURE 4-9

FRACTIONAL CHANGE IN THE PROPAGATION CONSTANT

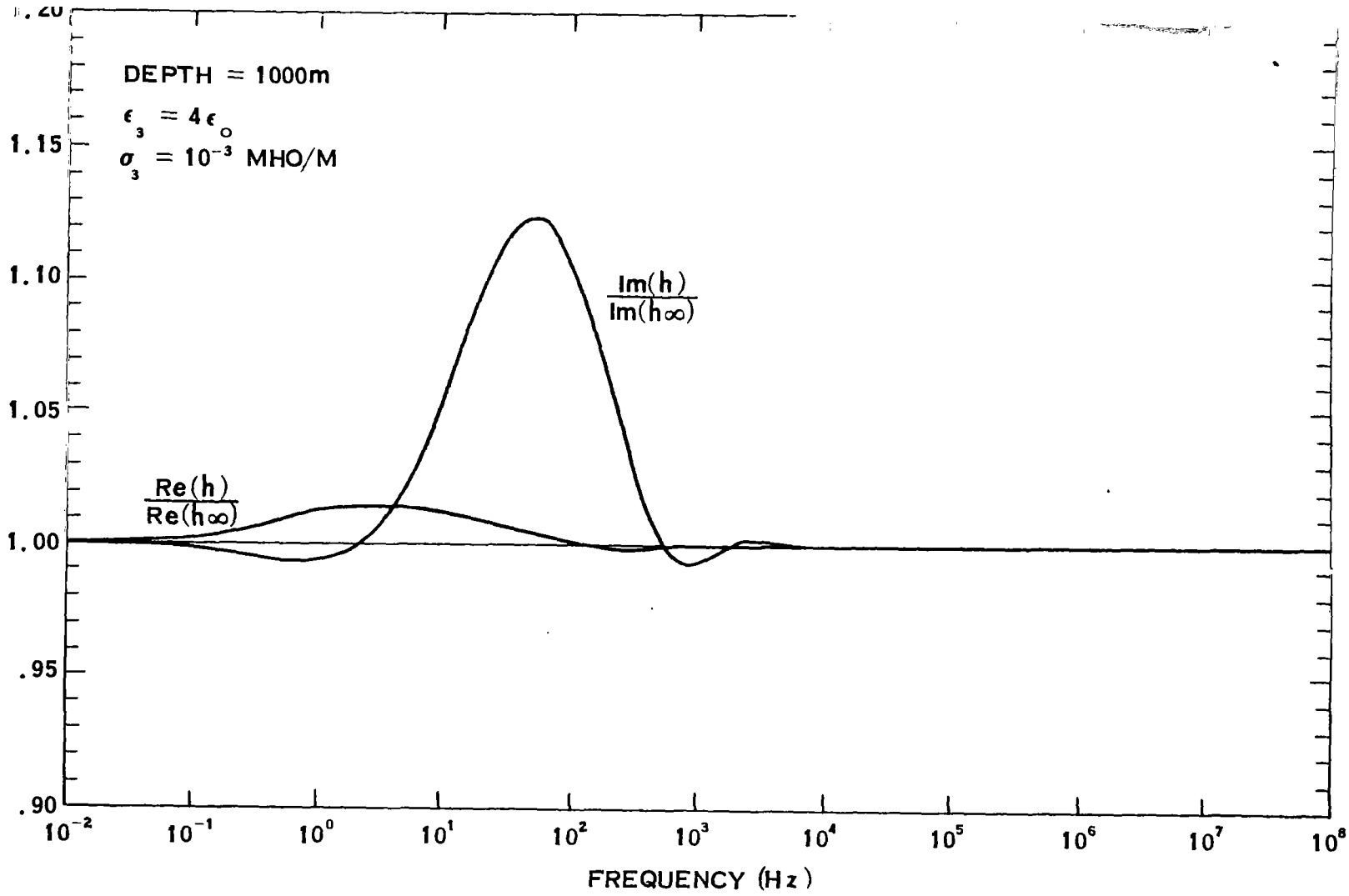

FIGURE 4–10

FRACTIONAL CHANGE IN THE PROPAGATION CONSTANT

As a comparison, Figure 4-11 shows the propagation constant determined with these variable parameters. Figure 4-12 through Figure 4-15 show the fraction change in h as a function of burial depth with σ_3 and ϵ_3 as given in Equation (4-1). The form of the results with frequency dependent soil parameters is essentially the same as the form of the results with the soil parameters listed in Table 1. The two sets of parameters give rise to differences in the details of the size of the change in h and the frequencies at which these changes occur.

The net effect of the air-earth interface on the propagation constant of a buried insulated conductor may be summarized as:

a) The imaginary part of h is decreased by ~2% at lower frequencies, but is dramatically increased (by as much as ~35%) at some characteristic frequency.

b) The real part of h is increased at lower frequencies by ~2%, followed by a decrease of as much as 10%.

c) At very low and very high frequencies, no variation of h is observed.

d) Both the magnitude of the change in the real and the imaginary parts of h, and the characteristic frequency at which these changes take place are reduced with increased burial depth.

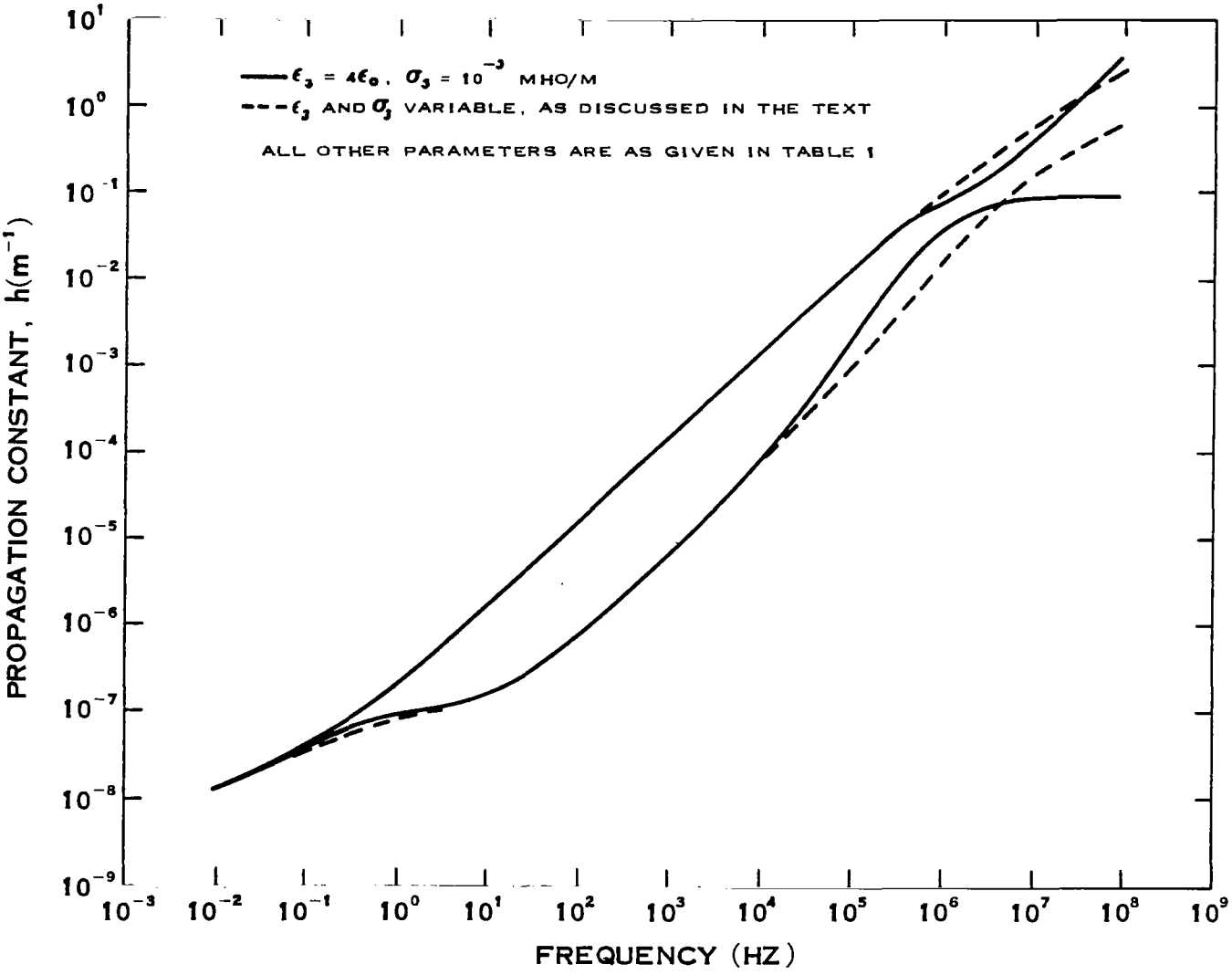

FIGURE 4—11

COMPARISON OF THE PROPAGATION CONSTANT (AT INFINITE BURIAL DEPTH) FOR DIFFERENT SOIL PARAMETERS.

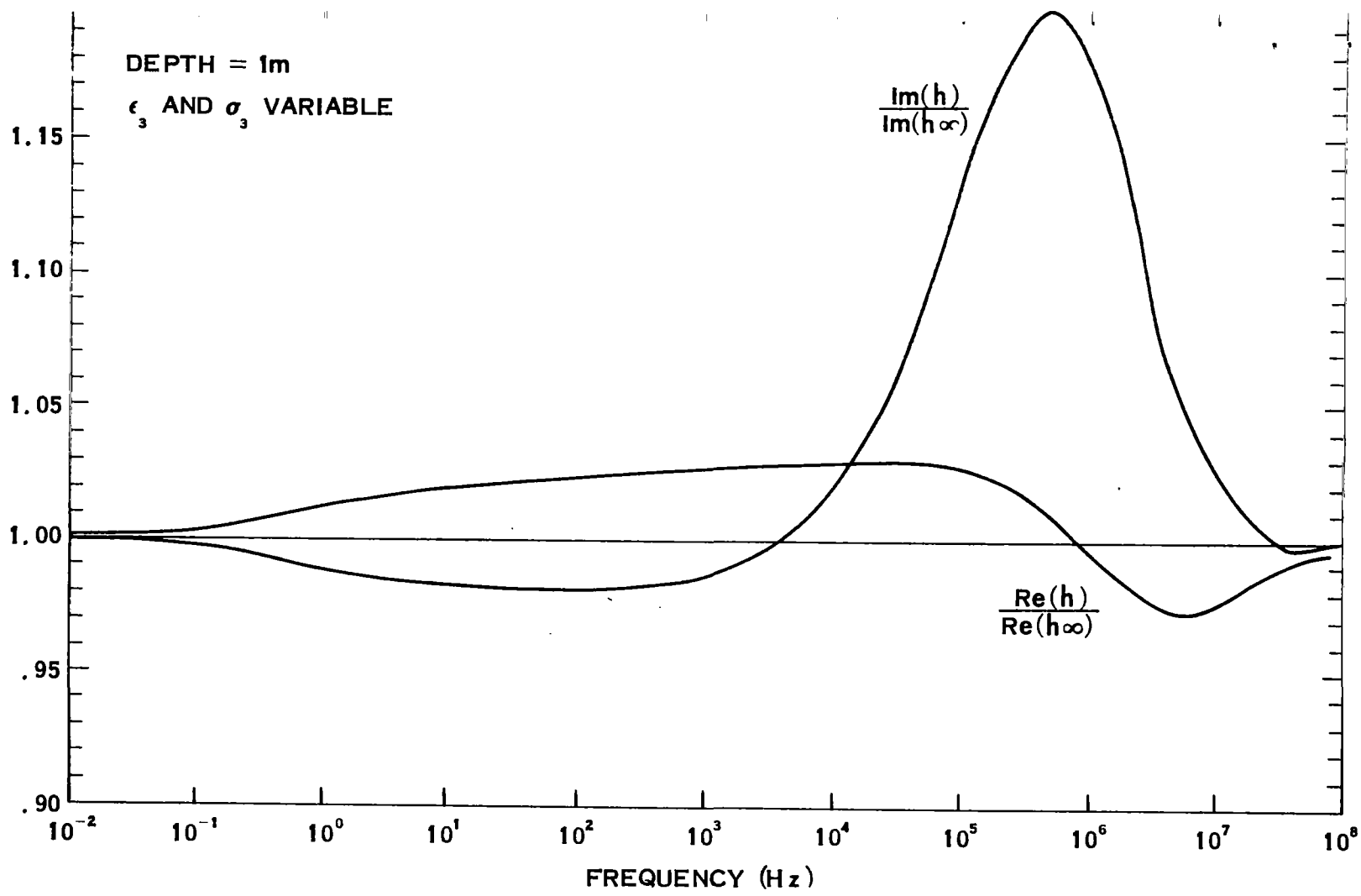

FIGURE 4–12

FRACTIONAL CHANGE IN THE PROPAGATION CONSTANT

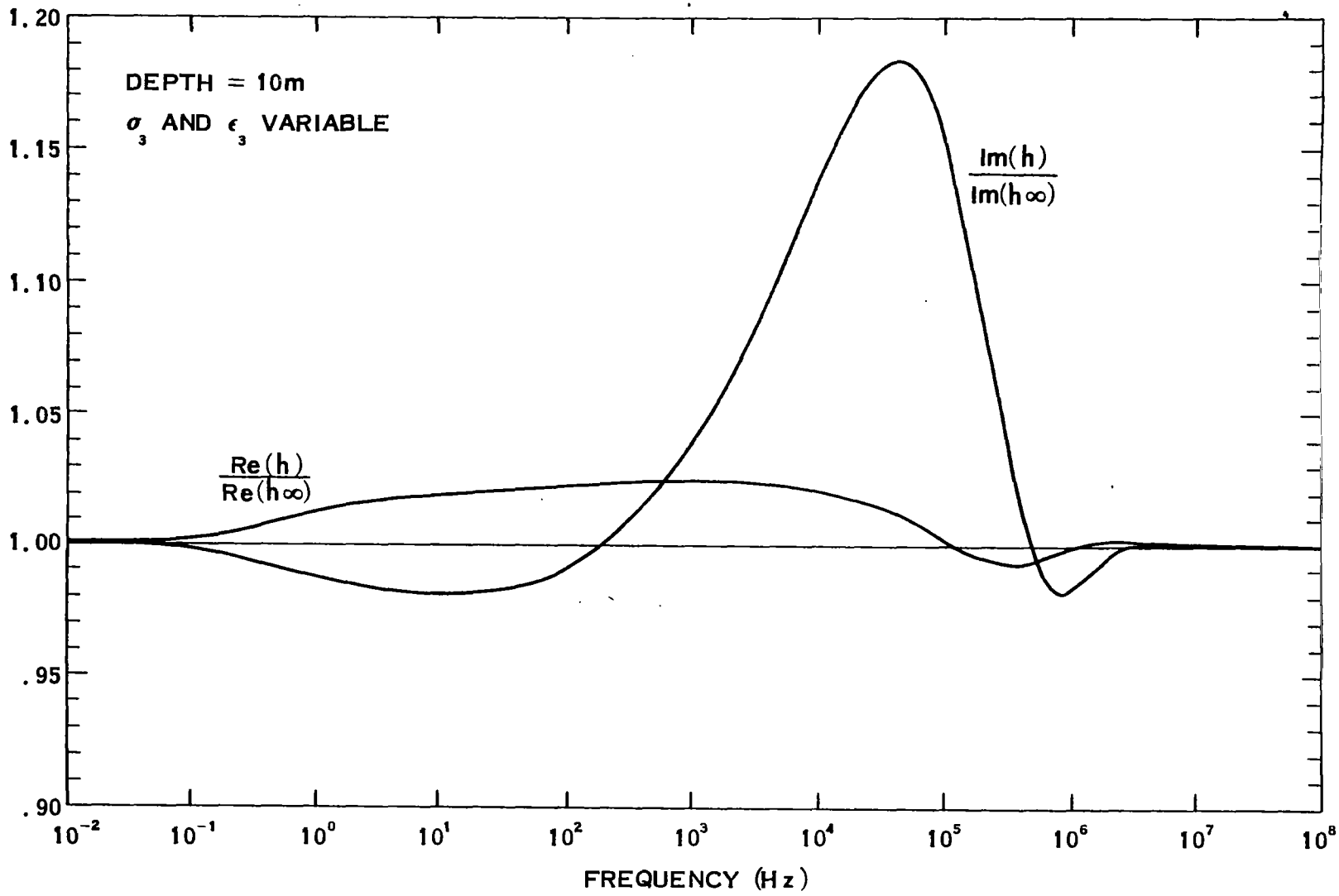

FIGURE 4–13

FRACTIONAL CHANGE IN THE PROPAGATION CONSTANT

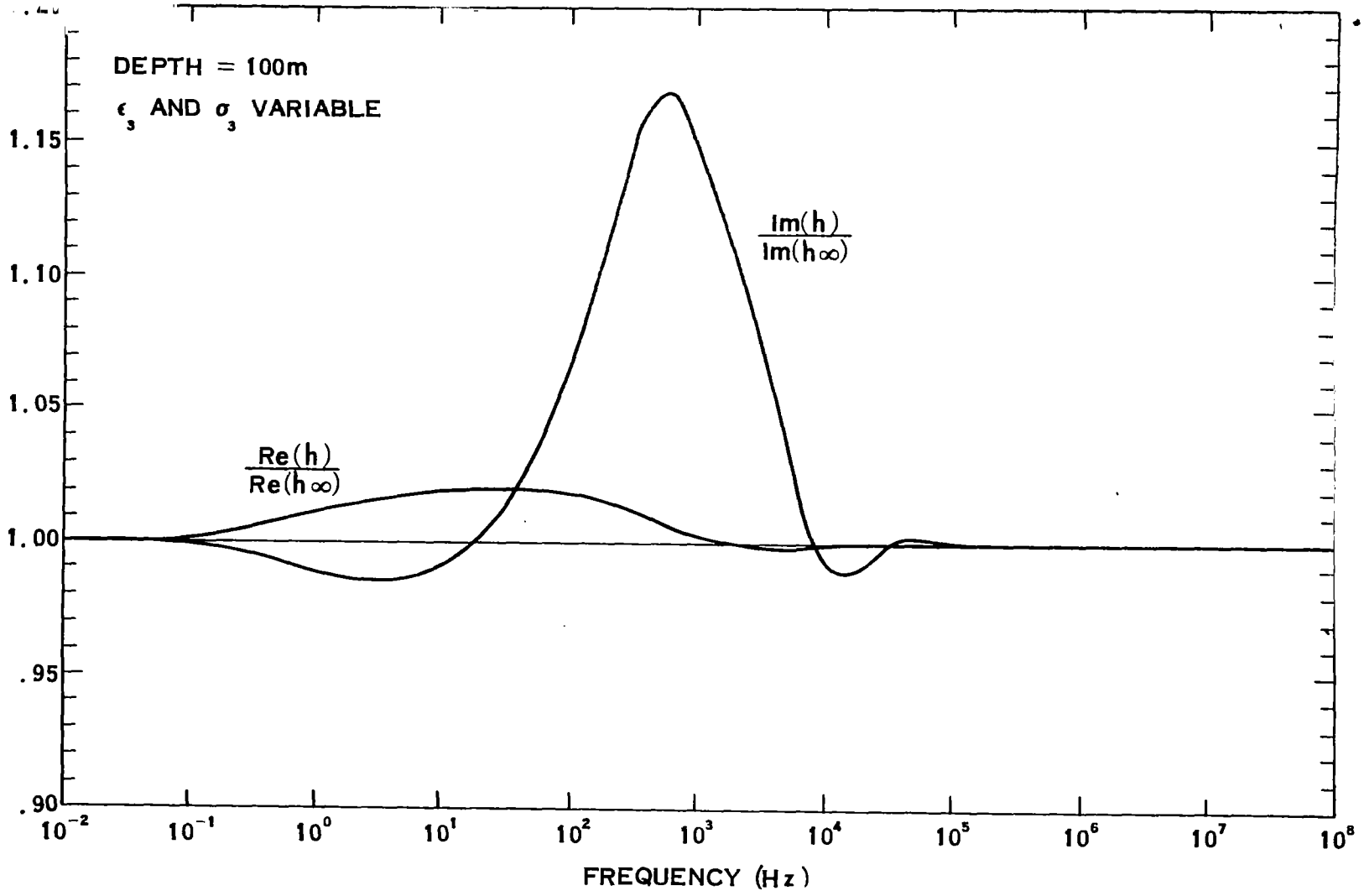

FIGURE 4-14

FRACTIONAL CHANGE IN THE PROPAGATION CONSTANT

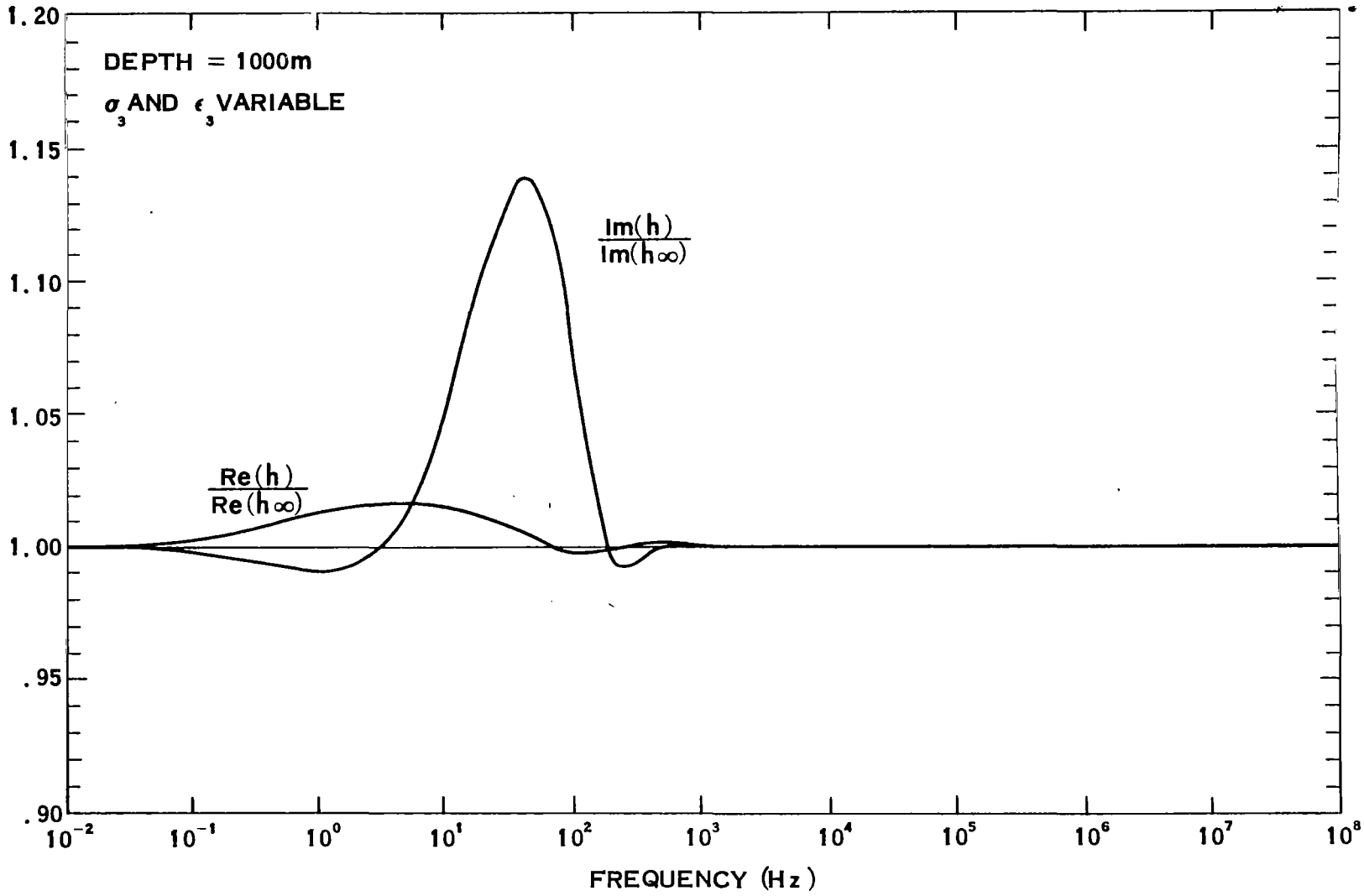

FIGURE 4–15

FRACTIONAL CHANGE IN THE PROPAGATION CONSTANT

APPENDIX A

A LOW FREQUENCY APPROXIMATE SOLUTION TO THE BURIED INSULATED CONDUCTOR

Under a variety of physical conditions, closed form, approximate solutions to Equations (2-27) and (2-28) may be obtained. These are permitted since the actual physical characteristics of a particular material may allow either small or large argument approximations to be made for some of the Bessel functions.

The case of particular interest is when medium (2) is a good insulator ($\sigma_2 = 0$), since for this case h is expected to be close to k_2, so that $\lambda_2^2 \equiv k_2^2 - h^2 < k_2^2 = \mu_2 \epsilon_2 \omega^2$. If μ_2 and ϵ_2 are the same order of magnitude as μ_o and ϵ_o, then $\lambda_2 \sim f/c$. Further since the cable dimensions are on the order of 10^{-2} meter, it can be said that $\lambda_2 r$ is a small number even for frequencies as high as $f = 10^8$ Hz. Consequently the following small argument expansions are permitted for all Bessel functions representing electric and magnetic fields in the insulator.

$$\rho << 1 \qquad \begin{aligned} J_o(\rho) &\simeq 1 \\ J_1(\rho) &\simeq \tfrac{1}{2}\rho \\ N_o(\rho) &\simeq -\frac{2}{\pi} \ln\left(\frac{2}{\gamma\rho}\right) \qquad \gamma = 1.78107 \\ N_1(\rho) &\simeq -\frac{2}{\pi}\,\frac{1}{\rho} \end{aligned} \qquad \text{(A-1)}$$

Using approximations (A-1), Equation (2-27) is solved for β:

$$\beta \simeq \frac{2}{\pi} \left[\ell n\left(\frac{2}{\gamma \lambda_2 a}\right) - \frac{\mu_1 \lambda_1 k_2^2}{\mu_2 \lambda_2^2 k_1^2 a} \cdot \frac{J_o(\lambda_1 a)}{J_1(\lambda_1 a)} \right] \qquad \text{(A-2)}$$

Similarly, an independent solution for β is obtained from Equation (2-28):

$$\beta \simeq \frac{2}{\pi} \left[\ell n\left(\frac{2}{\gamma \lambda_2 b}\right) - \frac{\mu_3 \lambda_3 k_2^2}{\mu_2 \lambda_2^2 k_3^2 b} \cdot \frac{H_o^{(1)}(\lambda_3 b)}{H_1^{(1)}(\lambda_3 b)} \right] \qquad \text{(A-3)}$$

Solutions (A-2) and (A-3) are equated, leaving a single equation to be solved for h, namely:

$$\ell n\left(\frac{2}{\gamma \lambda_2 a}\right) - \frac{\mu_1 \lambda_1 k_2^2}{\mu_2 \lambda_2^2 k_1^2 a} \cdot \frac{J_o(\lambda_1 a)}{J_1(\lambda_1 a)} \qquad \text{(A-4)}$$

$$\simeq \ell n\left(\frac{2}{\gamma \lambda_2 b}\right) - \frac{\mu_3 \lambda_3 k_2^2}{\mu_2 \lambda_2^2 k_3^2 b} \cdot \frac{H_o^{(1)}(\lambda_3 b)}{H_1^{(1)}(\lambda_3 b)} \quad .$$

Further since $\ell n\left(\frac{2}{\gamma \lambda_2 a}\right) - \ell n\left(\frac{2}{\gamma \lambda_2 b}\right) = \ell n(b/a)$, Equation (A-4) upon rearrangement reduces to

$$\left(\frac{\lambda_2}{k_2}\right)^2 \simeq \frac{1}{\mu_2 \ell n(b/a)} \left[\frac{\mu_1 \lambda_1}{k_1^2 a} \cdot \frac{J_o(\lambda_1 a)}{J_1(\lambda_1 a)} - \frac{\mu_3 \lambda_3}{k_3^2 b} \cdot \frac{H_o^{(1)}(\lambda_3 b)}{H_1^{(1)}(\lambda_3 b)} \right] \qquad \text{(A-5)}$$

For low frequency h is very small compared with either k_1 or k_3, so that $\lambda_1 \simeq k_1$, and $\lambda_3 \simeq k_3$. Under these approximations Equation (A-5) can be solved for the propagation constant directly.

$$h \simeq k_3 \left\{ 1 - \frac{1}{\mu_2 \ell n(b/a)} \left[\frac{\mu_1}{k_1 a} \cdot \frac{J_o(k_1 a)}{J_1(k_1 a)} - \frac{\mu_3}{k_3 b} \cdot \frac{H_o^{(1)}(k_3 b)}{H_1^{(1)}(k_3 b)} \right] \right\}^{\frac{1}{2}} \qquad \text{(A-6)}$$

The propagation constant, h, was calculated from solution (A-6) for a representative cable configuration. As shown in Figure 2-2, both the real and imaginary parts of h are in excellent agreement with the exact solutions to Equations (2-27) and (2-28) for the range of validity of the approximations ($f \lesssim 10^4$ Hz).

APPENDIX B

FRESNEL COEFFICIENTS

The electric fields of Equations (3-5) - (3-7) and their associated magnetic fields, found by applying Faraday's Law

$$\vec{H} = \frac{1}{i\mu\omega} \vec{\nabla} \times \vec{E} = \frac{1}{\mu\omega} \vec{k} \times \vec{E}, \qquad \text{(B-1)}$$

must satisfy the following boundary conditions at the air-earth interface:

1) The tangential electric field is continuous:

$$\hat{n} \times (\vec{E}_o + \vec{E}_R) = \hat{n} \times \vec{E}_T \qquad \text{(B-2)}$$

2) The tangential magnetic field is continuous:

$$\hat{n} \times (\vec{H}_o + \vec{H}_R) = \hat{n} \times \vec{H}_T$$

$$\Rightarrow \frac{1}{\mu_3} \hat{n} \times (\vec{k}_o \times \vec{E}_o + \vec{k}_R \times \vec{E}_R) = \frac{1}{\mu_4} \hat{n} \times (\vec{k}_T \times \vec{E}_T) \qquad \text{(B-3)}$$

3) The normal magnetic induction is continuous ($\vec{B} = \mu \vec{H}$)

$$\mu_3 \hat{n} \cdot (\vec{H}_o + \vec{H}_R) = \mu_4 \hat{n} \cdot \vec{H}_T$$

$$\Rightarrow \hat{n} \cdot (\vec{k}_o \times \vec{E}_o + \vec{k}_R \times \vec{E}_R) = \hat{n} \cdot (\vec{k}_T \times \vec{E}_T) \qquad \text{(B-4)}$$

4) The free charge deposited on the interface is given by

$$\hat{n} \cdot (\vec{D}_o + \vec{D}_R - \vec{D}_T) = \rho.$$

Further the current flowing through the interface is governed by the continuity equation

$$\hat{n} \cdot (\vec{J}_o + \vec{J}_R - \vec{J}_T) = - \frac{\partial \rho}{\partial t}$$

Since the time enters only through the common factor $e^{-i\omega t}$, and by Ohm's Law $\vec{J} = \sigma\vec{E}$, upon recognizing that $\vec{D} = \epsilon\vec{E}$ we have

$$\mu_4 k_3^2 \, \hat{n} \cdot (\vec{E}_o + \vec{E}_R) = \mu_3 k_4^2 \, \hat{n} \cdot \vec{E}_T \qquad \text{(B-5)}$$

There are two cases of polarization:

Case 1: $\vec{E}$ normal to plane of incidence

Equations (B-2) and (B-3) reduce to

$$E_{o_\perp} + E_{R_\perp} = E_{T_\perp} \qquad \text{(B-6)}$$

and

$$\frac{1}{\mu_3} (E_{o_\perp} k_{o_y} - E_{R_\perp} k_{o_y}) = \frac{1}{\mu_4} E_R \; k_{T_y} \qquad \text{(B-7)}$$

Equation (B-4) becomes identical to Equation (B-6) and Equation (B-5) vanishes. Thus

$$E_{R_\perp} = E_{o_\perp} \left\{ \frac{\mu_4 \, k_{o_y} - \mu_3 \, k_{T_y}}{\mu_4 \, k_{o_y} + \mu_3 \, k_{T_y}} \right\} \equiv f_{R_\perp} E_{o\perp} \qquad \text{(B-8)}$$

and,

$$E_{T_\perp} = E_{o_\perp} \left\{ \frac{2\mu_4 \, k_{o_y}}{\mu_4 k_{o_y} + \mu_3 k_{T_y}} \right\} \equiv f_{T_\perp} E_{o\perp} \qquad \text{(B-9)}$$

Case 2: $\vec{E}$ in the plane of incidence:

Equations (B-2) and (B-3) reduce to

$$\frac{k_{o_y}}{k_3}\left(E_{o_{||}} - E_{R_{||}}\right) = \frac{k_{T_y}}{k_4} E_{R_{||}} \tag{B-10}$$

and

$$\frac{k_3}{\mu_3}\left(E_{o_{||}} + E_{R_{||}}\right) = \frac{k_4}{\mu_4} E_{T_{||}} \tag{B-11}$$

Equation (B-4) vanishes and Equation (B-5) is identical with Equation (B-11). Thus

$$E_{R_{||}} = E_{o_{||}} \left\{ \frac{k_4^2 \mu_3 k_{o_y} - k_3^2 \mu_4 k_{T_y}}{k_4^2 \mu_3 k_{o_y} + k_3^2 \mu_4 k_{T_y}} \right\} \equiv f_{R_{||}} E_{o_{||}} \tag{B-12}$$

and,

$$E_{T_{||}} = E_{o_{||}} \left(\frac{k_4 \mu_3}{k_3 \mu_4}\right) \cdot \left\{ \frac{2k_4^2 \mu_3 k_{o_y}}{k_4^2 u_3 k_{o_y} + k_3^2 \mu_4 k_{T_y}} \right\} \equiv f_{T_{||}} E_{o_{||}} \tag{B-13}$$

The coefficients defined in Equations (B-8), (B-9), (B-12), and (B-13) are the Fresnel coefficients appearing in standard texts.[9] It is pointed out that there is a sign change in Equation (B-12) due to the particular coordinate system adopted (see Figure 3-2).

REFERENCES

1. Ware, W. E., et al, "EMP Induced Signals in Buried Linear Antennas (U)," Kaman Nuclear Report KN-785-69-49(R), 15 April 1969, SECRET.

2. Carson, J. R., "Wave Propagation in Overhead Wires with Ground Return," Bell Sys. Tech. J., Vol. 5, Oct. 1926, p. 539.

3. Guy, A. W., and Hasserjian, G.," Impedance Properties of Large Subsurface Antenna Arrays," IEEE Transactions on Antennas and Propagation, May 1963, p. 232.

4. Bannister, Peter R., "Electric and Magnetic Fields Near a Long Horizontal Line Source Above the Ground," Radio Science, Vol. 3 (New Series), p. 203; February 1968.

5. Wait, James R., "The Fields of a Line Source of Current Over a Stratified Conductor," Appl. Sci. Res., Sec. B, Vol. 3, p. 279; 1953.

6. Stratton, J. A., "Electromagnetic Theory," McGraw-Hill Book Co., Inc., New York, N. Y., 360-61; 1941.

7. Ware, W. E., et al, op. cit., Appendix E, p. E-1.

8. Erdélyi (editor), Tables of Integral Transforms, McGraw-Hill, 1.13(43), p. 56 (1954).

9. For example, J. A. Stratton, op. cit., pp. 493-494.